SLAC – PUB – 4352
June 1987
(T)

AN INTRODUCTION TO CHARM AND HEAVY QUARK PHYSICS*

Frederick J. Gilman

Stanford Linear Accelerator Center
Stanford University, Stanford, California 94305

Abstract The physics of the electroweak and strong interactions in the standard model are reviewed, especially as they apply to the tau lepton and to charm and heavy quark physics.

1. INTRODUCTION

Charm physics, as all other high energy physics, is now considered in reference to the framework of the standard model. The strong and electroweak interactions originate in gauge theories with the gauge group being $SU(3)_C \times SU(2) \times U(1)$, together with the assignment of fermions to triplets if they are quarks and singlets if they are leptons under $SU(3)_C$ and to left-handed doublets and right-handed singlets under the electroweak $SU(2)$. Given 18 or so parameters which are put in from outside the standard model, it is in excellent shape. Experiment has again and again confirmed its predictions to whatever accuracy they can be predicted and measured in a given situation. With the beginning of experiments at the Z factories in the near future, the one-loop corrections to the electroweak portion of the standard model will be tested to high accuracy.

* Work supported by the Department of Energy, contract DE–AC03–76SF00515.

Invited talks given at the Charm Physics Symposium
Beijing, China, June 4–16, 1987

While aware of the success of the standard model, we are also not satisfied with it as a final theory of Nature. It is incomplete. Many parameters, such as quark masses and weak mixing angles come, as noted above, from outside the standard model. Nor is the reason for quark and lepton families or generations explained, let alone a connection between quarks and leptons. Why are there 3 (?) generations? And then we have the hierarchy problem—how is a scale as "small" as the weak scale determined if we start at a grand-unified scale or at the Planck scale?

Therefore we are continually looking for evidence of the physics which must exist which is beyond or outside the standard model. We check and recheck with yet higher accuracy the predictions which follow from the standard model, hoping to find some hint of what lies beyond.

While working in what is now comparatively "low" energies, there are possibilities for physics discoveries at BEPC which could point beyond the standard model. Some examples which are of topical interest at the moment are:

- $D^0 - \bar{D}^0$ Mixing - This is a quantity which is small in the standard model, which makes it difficult to accumulate enough data to make a significant measurement, although present experiments are approaching the appropriate level.[1,2] By the same token, this is a good place to look for new physics. Where the standard effects are small (or even better, zero) is precisely where some new effect might stand out.[3]
- Measurement of $c \to d\bar{e}\nu$ as compared to $c \to s\bar{e}\nu$ Decays - Such measurements, if done accurately and combined with theoretical analysis, will permit the extraction of the ratio of

Kobayashi - Maskawa matrix elements V_{cd}/V_{cs}, if not their separate absolute values. This allows a check of unitarity of the three generation matrix using its second row (see the discussion in Section 2 for the first row).

- τ Decays - The search for "forbidden" (in the standard model) tau decays such as $\tau \to \mu\bar{e}e$, $\tau \to \mu K^0$, and $\tau \to \nu_\tau \eta\pi^-$ needs to be pushed to higher sensitivity. There is an intriguing problem, discussed in Section 4, that has arisen in the past few years as well of accounting for all the exclusive modes that make up the inclusive one-prong decays.

Both open and bound charm serve as a laboratory for standard model physics as well. To cite a few examples:

- Charmonium Spectroscopy - Charmonium presents a rich spectrum of narrow levels (see Figure 1) and has many photon and hadronic transitions which have been studied.[4] It is particularly interesting in comparison to light quark meson spectroscopy of $\bar{q}'q$ states and of bottomonium ($\bar{b}b$ states). It is non-relativistic enough ($v^2/c^2 \sim 0.3$) to apply a Schrodinger equation with an effective two-body potential, and thus to compare to the much more surely non-relativistic bottomonium case (see Figure 2). On the other hand, relativistic corrections are surely important in a number of cases and the charmonium system provides a kind of "bridge" between bottomonium and light quark mesons which are intrinsically relativistic by nature. The comparison of charmonium to other systems, and particularly bottomonium, is something I will stress repeatedly in Section 5, as we learn a great deal from this comparison and it gives us confidence in applying the lessons we learn in one system to another.

- $J/\psi \rightarrow \gamma +$ hadrons and $J/\psi \rightarrow \omega$ or $\phi +$ hadrons - These decays permit the high statistics study of light hadron spectroscopy and in particular the production of gluonium and "hybrid" ($\bar{q}qg$) states.[5] It clearly will form an essential part of the BEPC program.

- Weak Decays of D^+, D^0, D_s^+, and Λ_c^+ - Here we can see the interplay of the strong and weak interactions. We are again in a somewhat intermediate situation between K decays and B decays. In the latter case we expect the "spectator model" to work quite well, whereas we already know that there are corrections to it for charm, including the phenomena of final state interactions, color coherence, weak annihilation and Pauli interference which have been extensively discussed.[3]

2. THE STANDARD MODEL

The standard model for strong interactions, Quantum Chromodynamics (QCD), involves an unbroken $SU(3)_C$ gauge group with 8 gauge bosons, the gluons. These gauge bosons are coupled to the color charge carried by the the gluons themselves and by the quarks (and not leptons), which are assigned to the fundamental three dimensional representation of $SU(3)$.

Electroweak physics, on the other hand, is a gauge theory with the group structure $SU(2) \times U(1)$, spontaneously broken so as to have massive W^+, W^-, and Z vector bosons and a massless photon.[6] Within the gauge theory sector itself there are three parameters: g, the $SU(2)$ coupling; g', the $U(1)$ coupling; and the vacuum expectation value, v, of the Higgs field that is associated with spontaneous breaking of the continuous symmetry.

We usually do not work in terms of these three parameters. After defining the weak mixing angle through

$$\cos\theta_W = \frac{g}{(g^2+g'^2)^{1/2}}, \tag{1}$$

and identifying the electromagnetic coupling

$$e = g\sin\theta_W, \tag{2}$$

and the Fermi effective coupling

$$\frac{G_F}{\sqrt{2}} = \frac{g^2}{8\,M_W^2}, \tag{3}$$

with $M_W = gv/2$, it has been conventional to use $\alpha = e^2/4\pi$, G_F and $\sin^2\theta_W$ as the three parameters of the theory. This is related to the very accurate experimental determinations of the first two, α and G_F, leaving $\sin^2\theta_W$ to be pinned down as the characteristic parameter expressing the unification of weak and electromagnetic interactions. The W and Z boson masses are related by

$$M_W = M_Z\cos\theta_W, \tag{4}$$

and the W mass itself, using Eqs. (2) and (3) in lowest order, is given numerically by

$$M_W = \frac{37.3\ \text{GeV}}{\sin\theta_W}. \tag{5}$$

(Electroweak radiative corrections change this to $M_W = 38.65\ \text{GeV}/\sin\theta_W$.) While up to the present it is $\sin^2\theta_W$ that is commonly used as the third parameter, Eqs. (4) and (5) make it clear that

we could use M_W or M_Z. Until their discovery, this made no sense, but already the experimental uncertainty on their masses gives a comparable accuracy in the determination of $\sin^2\theta_W$ to that from measurements in low energy neutral current experiments.[7] In fact, once we enter the era of Z physics, it is much more appropriate to use α, G_F, and M_Z as the three parameters of the electroweak gauge theory, since M_Z will be fairly easily measured to an accuracy which will far exceed its equivalent in other determinations of $\sin^2\theta_W$.

The fermions in the standard model of electroweak interactions are assigned to left-handed doublets and right-handed singlets, thereby fixing their couplings to the gauge bosons of the electroweak interactions. For example, the charged W is coupled to $\bar{e}\nu_e$ with $g_V = -g_A = g/2\sqrt{2}$ and the Z is coupled to $\bar{\nu}\nu$ with $g_V = g_A = g/4\cos\theta_W$.

For the quark sector, there is the additional complication that the weak and mass eigenstates are not the same. The Kobayashi - Maskawa matrix[8] is defined as the matrix transformation that takes us from the mass eigenstates of the d, s, and b quarks to the weak eigenstates, d', s', and b', the partners in weak doublets of the u, c, and t quarks, respectively, which by convention are unmixed:

$$\begin{pmatrix} d' \\ s' \\ b' \end{pmatrix} = \begin{pmatrix} V_{ud} & V_{us} & V_{ub} \\ V_{cd} & V_{cs} & V_{cb} \\ V_{td} & V_{ts} & V_{tb} \end{pmatrix} \begin{pmatrix} d \\ s \\ b \end{pmatrix} . \qquad (6)$$

The 1986 Review of Particle Properties[9] gave the following results for the magnitudes of those matrix elements that can be measured up to the present time:

(1) Nuclear beta decay, when compared to muon decay, gave

$$|V_{ud}| = 0.9729 \pm 0.0012 .$$

which included refinements[10] which had lowered $|V_{ud}|$ by 0.13%.

(2) Analysis[11] of hyperon and K_{e3} decays yielded

$$|V_{us}| = 0.221 \pm 0.002 \ .$$

(3) From ν and $\bar{\nu}$ production of charm, the CDHS group[12] had deduced

$$|V_{cd}| = 0.24 \pm 0.03 \ .$$

(4) By comparing the experimental value[13] for $\Gamma(D \to \overline{K} e^+ \nu_e)$ with the expression that follows from the standard weak interaction amplitude, one derives:

$$|f_+^D(0)|^2 |V_{cs}|^2 = 0.51 \pm 0.07 \ .$$

where f_+^D is the form factor for $D_{\ell 3}$ decay which is the analogue of f_+ for $K_{\ell 3}$ decay. With the conservative assumption that $|f_+(0)| < 1$,

$$|V_{cs}| > 0.66 \ .$$

(5) The ratio $|V_{ub}/V_{cb}|$ is obtained from the semileptonic decay of B mesons by fitting to the lepton energy spectrum as a sum of contributions involving $b \to u$ and $b \to c$. As more data had accumulated, the inadequacy of previous parametrizations of the lepton spectrum became clear.[6] Using only the lepton momentum region beyond the end-point for $b \to c\ell\overline{\nu}_\ell$ resulted in[6]

$$\Gamma(b \to u\ell\overline{\nu}_\ell)/\Gamma(b \to c\ell\overline{\nu}_\ell) < 0.08 \ ,$$

which translates to

$$|V_{ub}/V_{cb}| < 0.19 \ .$$

(6) The magnitude of V_{cb} itself can be determined if the measured semileptonic bottom hadron partial width is assumed to be that of a b quark decaying through the usual $V - A$ interaction

(which from (5) is $BR(b \to c\ell\overline{\nu}_\ell)$ to within 8%):

$$0.037 < |V_{cb}| < 0.053 \ .$$

One can not prove there are three generations from these data, but only show consistency with that as a hypothesis. The crucial test at present comes from the constraint which unitarity of the 3×3 matrix imposes on the first row:

$$(0.9729 \pm 0.0012)^2 + (0.221 \pm 0.002)^2 + (< 0.01)^2 = 0.9954 \pm 0.0025, \tag{7}$$

with a couple of standard deviations from unity of the right hand side being insufficient to make a fuss about.

Since the Review of Particle Properties went to press, there have been some small shifts in the central values of some of the matrix elements due to reanalysis and/or new data, such as incorporating newer charm semileptonic branching ratios in extracting[14] $|V_{cs}|$. More importantly, a change[15] in the order $Z\alpha^2$ Coulomb corrections brought different experiments into better agreement and raised the value of $|V_{ud}|$:

$$|V_{ud}| = 0.9747 \pm 0.0010,$$

to be compared with a very recent result[16]

$$|V_{ud}| = 0.9755 \pm 0.0017,$$

which also improves on previous analyses of this quantity, primarily in terms of the electron screening correction.[17] The unitarity sum for the first row is now 0.9989 ± 0.0021 or 1.0004 ± 0.0035, depending on which new result one uses. One couldn't ask for better agreement with three generations. Turning this around, and using unitarity to restrict the coupling between the u quark and a new charge $-1/3$

quark results in

$$|V_{ub'}| \leq 0.06. \tag{8}$$

This is not very restrictive and, looking at its primary origin in the error bar on $|V_{ud}|$, it seems unlikely that there will be a very significant improvement upon it in the future.

3. WEAK DECAYS OF HEAVY QUARKS

This is a subject which is comparatively new, but one which is already in a fairly mature state experimentally:[1,2] we have measurements of many D meson branching ratios, including Cabibbo suppressed nonleptonic modes and the decomposition of the semileptonic decays into exclusive channels; excellent lifetime measurements exist for both charm and bottom hadrons; a good beginning has been made on the study of exclusive decays of the D_s, Λ_c and $B^{0,+}$.

On the theoretical side, we have a solid general framework within which to calculate these weak decays. In particular, this means starting with the electroweak interactions and their gauge group, $SU(2) \times U(1)$, and adding the corrections due to the strong interactions through the use of the renormalization group equation (or an equivalent formulation of the same physics), with anomalous dimensions computed from QCD.

These calculations are carried out at the quark level. A first stage in their application to actual hadrons is simply to neglect any other constituent of the decaying hadron aside from the heavy quark. In such a spectator model, as it is called, one directly carries over the quark level calculation to be the hadron level result, with the spectator quarks and gluons assumed to arrange themselves into the

final state particles together with the quarks (or leptons) coming from the heavy quark at no cost or benefit to the overall rate.

From the present data on charmed particle lifetimes, it is clear that there are differences of a factor of two or so between different species.[1,2] To understand this theoretically, it is necessary to go beyond the spectator model and to consider not just what happens at the quark level but at the hadron level. In so doing, ideas such as annihilation diagrams, interference, color (mis)matching, and final state interactions have entered the discussion.[18]

We give here only an introduction to the subject of the decays of hadrons containing heavy quarks. We will work at the quark level, where we know quite precisely how to proceed theoretically and the results give a semi-quantitative description of the experimental situation as we know it today. The corrections to the spectator model and the detailed analysis of the approaches to a full understanding of weak charm decays are found elsewhere.[18]

- Semileptonic Decays

It is theoretically simplest to start with semileptonic decays of the form

$$Q \to q + e\bar{\nu}_e$$

(such as $b \to ce\bar{\nu}_e$) or

$$Q \to q + \bar{e}\nu_e$$

(such as $c \to s\bar{e}\nu_e$) which correspond to a Hamiltonian density of the

form

$$\mathcal{H} = -V_{Qq} \frac{G_F}{\sqrt{2}} \bar{q}\gamma_\mu(1-\gamma_5)Q \; \bar{e}\gamma^\mu(1-\gamma_5)\nu_e. \tag{9}$$

In Eq. (9) we have used particle names in place of the corresponding spinor operators and introduced the one factor that does not enter into the analogous expression for muon decay, the Kobayashi - Maskawa matrix element V_{Qq}.

The corresponding decay rate can then be easily related to that for muon decay, $G_F^2 m_\mu^5/192\pi^3$:

$$\Gamma(Q \to qe\bar{\nu}_e) = |V_{Qq}|^2 \frac{G_F^2 M_Q^5}{192\pi^3} F\left(\frac{m_q}{M_Q}\right) \tag{10}$$

where

$$F(\Delta) = 1 - 8\Delta^2 + \Delta^6 - \Delta^8 - 24\Delta^4 \ell n \Delta. \tag{11}$$

Note again the extra Kobayashi - Maskawa factor in front and the phase space factor, $F(\Delta)$, which is unity for a massless final quark ($\Delta = 0$). This factor drops off rather quickly, so that $F(0.3) = 0.52$, a value relevant approximately for the $c \to s$ and the $b \to c$ transitions.

The electron (positron) energy spectrum is different in the two cases. For $b \to ce\bar{\nu}_e$ it is like that in muon decay and gives rise to a "hard" spectrum that does not vanish at the high energy end:

$$\frac{1}{\Gamma}\frac{d\Gamma}{dx} = \frac{12}{5} x^2(2-x), \tag{12}$$

while for $c \to s\bar{e}\nu_e$ (and for $t \to b\bar{e}\nu_e$) it vanishes at the two ends

$$\frac{1}{\Gamma}\frac{d\Gamma}{dx} = 12x^2(1-x) \tag{13}$$

where the scaled energy variable is

$$x = \frac{2E_e}{M_Q} \leq 1 - \frac{m_q^2}{M_Q^2}. \tag{14}$$

Similar results of course hold for decays involving muons or taus.

- Nonleptonic Decays

The Hamiltonian density for nonleptonic decays such as $Q \to q + u\bar{d}$ has the same basic form,

$$\mathcal{H} = -V_{Qq} \frac{G_F}{\sqrt{2}} \bar{q}_\alpha \gamma_\mu (1 - \gamma_5) Q_\alpha \; \bar{u}_\beta \gamma^\mu (1 - \gamma_5) d_\beta \tag{15}$$

as for semileptonic decays, aside from the addition of the color indices α and β which are summed over the three colors to form color singlet currents. The decay rate

$$\Gamma(Q \to qu\bar{d}) = 3 \;\; |V_{Qq}|^2 \; \frac{G_F^2 M_Q^5}{192\pi^3} \; F\left(\frac{m_q}{M_Q}\right) \tag{16}$$

is also identical to the semileptonic case except for the factor of three on the right hand side due to color (we are neglecting the masses of the u and d quarks, just as we neglected those of the e and ν_e previously).

Now let us rewrite the Hamiltonian in a slightly different form:

$$\begin{aligned}\mathcal{H} = -V_{Qq}\,\frac{G_F}{2\sqrt{2}}\cdot \\ \Big[c_+\Big[\bar{q}_\alpha\gamma_\mu(1-\gamma_5)Q_\alpha\bar{u}_\beta\gamma^\mu(1-\gamma_5)d_\beta \\ + \bar{q}_\alpha\gamma_\mu(1-\gamma_5)d_\alpha\bar{u}_\beta\gamma^\mu(1-\gamma_5)Q_\beta\Big] \\ + c_-\Big[\bar{q}_\alpha\gamma_\mu(1-\gamma_5)Q_\alpha\bar{u}_\beta\gamma^\mu(1-\gamma_5)d_\beta \\ - \bar{q}_\alpha\gamma_\mu(1-\gamma_5)d_\alpha\bar{u}_\beta\gamma^\mu(1-\gamma_5)Q_\beta\Big]\Big]\end{aligned} \tag{17}$$

with $c_+ = c_- = 1$ initially. All we have done is to add and subtract a term which is nothing but the original expression with $Q \leftrightarrow d$. Moreover, this term would be identical to the original one if it were not for the presence of the color indices; without them the interchange $Q \leftrightarrow d$ is a Fierz transformation under which $V - A$ interactions go into themselves. In the decay rate, the three on the right-hand side of Eq. (16) is replaced by $2c_+^2 + c_-^2$, which again is no change at all when $c_+ = c_- = 1$.

So why make a more complicated expression out of something simple? The answer lies in what happens when we turn on the strong interactions and add the effects of QCD to the purely weak interactions that we have considered up to this point. The weak interaction will be modified by the presence of strong interaction effects and c_+ and c_- will be renormalized. But they have been carefully chosen in this regard, for they only go into themselves under this renormalization, i. e. the corresponding operators, which are even or odd under interchange of color indices, do not mix through QCD corrections. Not only do the strong interactions modify c_+ and c_- from

their initial value of unity, but they introduce new operators into the effective Hamiltonian. These so-called "penguin" operators, which come in beginning at the one loop level, have a different space-time structure than the $V-A \times V-A$ structure we have had up to now. We proceed to consider each of these effects and their magnitude in turn.

- The Calculation of c_+ and c_-

Calculating what happens to c_+ and c_- under renormalization due to QCD is equivalent to studying their behavior as one moves from one momentum scale to another. More specifically, at the momentum scale corresponding to M_W the weak interactions are characterized by the "bare" Hamiltonian density of Eq. (15) and $c_+ = c_- = 1$. We are interested in what happens when we move down to a momentum scale of relevance to a particular hadron, *i.e.*, roughly the mass of the decaying heavy quark.

The study of what happens when one moves from one momentum scale to another is directly formulated through a renormalization group equation. In the case of c_+ and c_-, they satisfy such an equation of the form:

$$\left[\mu\frac{\partial}{\partial\mu} + \beta(g)\frac{\partial}{\partial g} - \gamma_\pm(g)\right] c_\pm(q/\mu, g) = 0, \qquad (18)$$

where μ is some reference scale of momentum (the renormalization point) and q is a second scale at which we wish to calculate the effective weak Hamiltonian. In this equation, $\beta(g)$ is the standard beta function of the theory,

$$\beta \equiv \mu\frac{\partial g}{\partial\mu},$$

which characterizes how the coupling changes with a change of scale. For QCD, it has the perturbation theory expansion,

$$\beta(g) = \frac{g^3}{48\pi^2}(2n_f - 33) + ... \tag{19}$$

where n_f is the number of quark flavors. Notice that the coefficient of g^3 is negative as long as $33 > 2n_f$. In other words, the coupling decreases as we increase the scale of momentum at which we are looking. This is just the property of asymptotic freedom; the theory of QCD becomes more and more like a free field theory as we increase the momentum scale. The quantities $\gamma_\pm$ are the anomalous dimensions associated with the operators $c_\pm$, respectively. They also can be calculated in a perturbative expansion, starting in order g^2, where they originate in graphs where a single gluon is exchanged between fermion lines in the basic four-fermion weak interaction:[19]

$$\gamma_+ = +\frac{g^2}{4\pi^2} + ... \tag{20a}$$

$$\gamma_- = -\frac{g^2}{2\pi^2} + ... \tag{20b}$$

Note that if $\gamma_\pm = 0$, then the combination of derivatives on the left-hand side of the renormalization group equation can be rewritten as a total derivative:

$$\left[\mu\frac{\partial}{\partial\mu} + \beta(g)\frac{\partial}{\partial g}\right] c_\pm(q/\mu, g) = \left[\mu\frac{d}{d\mu}\right] c_\pm = 0, \tag{21}$$

simply expressing the fact that $c_\pm$ does not change under a change of momentum scale if the anomalous dimensions are zero. In the case at hand, as we have just seen, the anomalous dimensions are non-zero and the operator coefficients $c_\pm$ change with scale.

We now proceed to solve this renormalization group equation.[20] The method of solution that follows looks like it is pulled out of the hat, but bear with me.

We begin by defining the quantity $\bar{g}$ through an integral:

$$\ln(q/\mu) \equiv \int_{g}^{\bar{g}(q/\mu,g)} \frac{dx}{\beta(x)} \tag{22}$$

with $\bar{g}(1,g) = g$. The quantity $\bar{g}$, which is dimensionless, can only be a function of the ratio of the momentum scales q and μ and the coupling g at the reference scale μ; it is just the "running coupling" that is familiar to all of us. To see this, let us put it in a more familiar form by looking at the situation when $\bar{g}$ is small, so that we can use the perturbative result for $\beta(x) = \frac{x^3}{48\pi^2}(2n_f - 33) + ...$ under the integral in Eq. (22). If we take the first term in this expansion we obtain on performing the integral,

$$\ln q/\mu = \frac{48\pi^2}{2n_f - 33}\frac{1}{2}\left(\frac{1}{g^2} - \frac{1}{\bar{g}^2}\right) \tag{23}$$

or

$$\alpha_s(q^2) \equiv \frac{\bar{g}^2}{4\pi} = \frac{\alpha_s(\mu^2)}{1 + \frac{33-2n_f}{12\pi}\alpha_s(\mu^2)\ln q^2/\mu^2}. \tag{24}$$

This is the standard expression for the running of α_s when it is small.

The definition of $\bar{g}$ in Eq. (22) is perfectly general; it simply reduces to the standard form in the small coupling region upon using lowest order perturbation theory for $\beta(x)$. Moreover, it is relevant to solving our equation since it exactly satisfies the renormalization

group equation with zero anomalous dimensions:

$$\left(\mu\frac{\partial}{\partial\mu}+\beta(g)\frac{\partial}{\partial g}\right)\bar{g}(q/\mu,g)=0, \tag{25}$$

as may be seen by applying the differential operator on the left-hand side of this equation to both sides of Eq. (22).

Now we are ready to solve the full equations for $c_\pm$. The solution of Eq. (18) is:

$$c_\pm(q/\mu,g)=c_\pm(1,\bar{g})\exp\left(\int_g^{\bar{g}}-\frac{\gamma_\pm(x)dx}{\beta(x)}\right), \tag{26}$$

as can be seen directly by substitution and employing Eq. (25) together with the fact that the derivative of an integral with respect to its upper limit of integration is just the integrand evaluated at that point.

We go again to perturbation theory to evaluate the integral in the exponent of Eq. (26):

$$\int_g^{\bar{g}}-\frac{\gamma_+(x)dx}{\beta(x)}=\frac{6}{33-2n_f}\ln\frac{\bar{g}^2}{g^2}. \tag{27}$$

Therefore,

$$c_+(q/\mu,g)=c_+(1,\bar{g})\left(\frac{\bar{g}^2}{g^2}\right)^{\frac{6}{33-2n_f}}, \tag{28}$$

and similarly,

$$c_-(q/\mu,g)=c_-(1,\bar{g})\left(\frac{\bar{g}^2}{g^2}\right)^{\frac{-12}{33-2n_f}}. \tag{29}$$

We are interested in what happens between a momentum scale

which is characteristic of the decaying hadron (which we take to be μ) and the weak scale, M_W (which we take to be q). Moreover, if we had also taken our reference momentum scale μ to be the weak scale, our coefficients should make the Hamiltonian density correspond to the "bare" density in Eq. (17), *i.e.*, $c_\pm(1,\bar{g}) = 1$. Therefore,

$$c_+(M_W/\mu, g) = \left(\frac{\alpha_s(M_W^2)}{\alpha_s(\mu^2)}\right)^{\frac{6}{33-2n_f}} \tag{30}$$

and

$$c_-(M_W/\mu, g) = \left(\frac{\alpha_s(M_W^2)}{\alpha_s(\mu^2)}\right)^{\frac{-12}{33-2n_f}}. \tag{31}$$

This, finally, is our long-sought result for the coefficients $c_\pm(M_W/\mu, g)$.

When we recall that $\alpha_s(q^2)$ runs down as the momentum scale goes up, we see that $c_+(M_W/\mu, g) < 1$ and $c_-(M_W/\mu, g) > 1$. In fact, there is the simple relation

$$c_+^2 c_- = 1 \tag{32}$$

(which is traceable to the factor of -2 between the anomalous dimensions of the corresponding operators), so that one of the corresponding terms in the weak Hamiltonian is necessarily suppressed if the other is enhanced by the effects of QCD.

- Penguins

Before using these results to look at the overall picture of decays in the spectator model, let us take a brief look at the additional operators introduced by QCD, the "penguins". A set of lowest order graphs which contribute to the existence of "penguin" operators relevant to various quark decays is shown in Figure 3.

On the upper left is a one loop, "penguin" graph relevant to strange quark decay (and in particular, to neutral K decay). Once the loop integral is performed this diagram contributes to an effective operator whose space-time structure is $(V-A)\times V$, or equivalently a mixture of $(V-A)\times(V-A)$ and $(V-A)\times(V+A)$. The latter operator has a structure that is not in the original weak Hamiltonian density. Arguments have been made that although its relative coefficient is small, the corresponding operator has a big matrix element in K decays and that it contributes a large part of the experimentally observed amplitude.[21] This is a subject still very much under debate.[22]

The diagram on the upper right shows a potential "penguin" in Cabibbo suppressed charm decays. Estimates generally put its strength well below that from ordinary graphs which contribute to the same process.

In bottom decay, however, it may be possible to have processes (Cabibbo suppressed to be sure) where "penguin" diagrams give rise to contributions comparable to, or maybe even larger than, those of ordinary tree level graphs.[23] The bottom portion of Figure 3 shows a possible example. The "penguin" diagram on the lower left contributes an effective Hamiltonian density:

$$\mathcal{H} = \frac{G_F}{\sqrt{2}}\frac{\alpha_s}{3\pi}\, V_{tb}\, V_{ts}^*\, \ln(m_t^2/m_c^2)\; \bar{s}\gamma_\mu(1-\gamma_5)b\bar{u}\gamma^\mu u, \qquad (33)$$

whereas the usual spectator diagram (aside from factors of $c_\pm$, which are close to unity) corresponds to

$$\mathcal{H} = \frac{G_F}{\sqrt{2}}\, V_{ub}\, V_{us}\; \bar{u}\gamma_\mu(1-\gamma_5)b\; \bar{s}\gamma^\mu(1-\gamma_5)u. \qquad (34)$$

The "penguin" loses to the spectator graph because of the

$\frac{\alpha_s}{3\pi}\ln(m_t^2/m_c^2)$ that arises from having one loop and the presence of the gluon, but it wins because of the Cabibbo (or more exactly, Kobayashi-Maskawa) factor $V_{tb}V_{ts}^*$, which involves zero and one generation jumps, as compared to $V_{ub}V_{us}$, which involves two and one generation jumps, respectively. Depending in part on how small V_{ub} is (something still not known), it could well be that the spectator graph gives the lesser of the two contributions. Then, for example, in the decays $B_d \to K^+\pi^-$ or $B_s \to \phi K^0$ the "penguin" contribution may be dominant.[24]

- Decays in the Spectator Model

What does all this mean numerically for the decay of the various quark flavors? First consider the strange quark. The statement that $c_- > 1$ corresponds to the enhancement of the $\Delta I = 1/2$ amplitude in strange particle decay, which is what one desires in order to be in accord with experiment. However, it already requires some stretching to get a factor of 3 or 4 in the amplitude, while what is needed is something like a factor of 20. Another piece of physics, perhaps "penguins" (see the discussion above), is required in addition to the QCD enhancement of c_-.

For the charm quark, if we set $\mu = m_c$, we find $c_- \sim 2$ and $c_+ \sim 1/\sqrt{2}$. At the quark level the Cabibbo allowed decay channels are $c \to s\bar{e}\nu_e$, $c \to s\bar{\mu}\nu_\mu$, and $c \to s\bar{d}u$. In the spectator model, all charmed hadrons would have the same lifetime and the same semileptonic branching fraction, which would be identified with that for the charm quark as if it decayed in isolation from other hadronic constituents:

$$BR_{\text{semileptonic}} \sim \frac{1}{2 + 2c_+^2 + c_-^2} \sim 14\%. \tag{35}$$

For the bottom quark, with $\mu = m_b$, the QCD enhancement (suppression) of c_- (c_+) is less than that for charm: $c_- \sim 1.5$ and $c_+ \sim 0.8$. In this case we have an expanded list of decay channels at the quark level: $b \to ce\bar{\nu}_e$, $b \to c\mu\bar{\nu}_\mu$, $b \to c\tau\bar{\nu}_\tau$, $b \to cd\bar{u}$, and $b \to cs\bar{c}$. We have neglected decays where the final c quark is replaced by a u quark (using the experimental result[1] that $b \to u/b \to c$ is small). The corresponding semileptonic branching ratio is

$$BR_{\rm semileptonic} \sim \frac{1}{2.2 + 1.2(2c_+^2 + c_-^2)} \sim 15\%, \qquad (36)$$

where the semileptonic decays involving $c\bar{\tau}\nu_\tau$ and $c\bar{c}s$ have been given an approximate phase space weight which is 0.2 times that for $c\bar{e}\nu_e$.

On the one hand, as noted at the beginning of this Section, these results do not agree with experiment, e.g., the D^0 and the D^+ lifetimes differ by a factor of two or so, the average B semileptonic branching ratio is about 12%, *etc.*[1,2] On the other hand, before fixing up the shortcomings of the spectator model,[18] I emphasize that this is not so bad – I only wish that I was able to calculate so simply everything else involving strong interactions to a factor of two or better in the rate! The spectator model provides a semi-quantitative basis for calculating the weak decays of heavy quarks, and is the starting point for the improvements needed to obtain a detailed understanding when we take into account the effects of the other quarks and gluons present in the initial or final state.

4. THE TAU LEPTON

All the properties of the tau are consistent with its being a third generation lepton, *i.e.*, just another copy of the electron and muon,

albeit much heavier.[25] The front-back asymmetry measurements in $e^+e^- \to \mu^+\mu^-$ determine the g_A coupling of the Z to $\bar{\tau}\tau$ so as to make the tau the lower component of a weak doublet. The other member of the $SU(2)$ doublet, the tau neutrino, must be distinct from the electron and muon neutrinos. The upper bound on the tau neutrino mass has been lowered to 70 MeV, below the mass of the charged lepton of the previous generation.[26]

The recent measurement of the charged lepton momentum spectrum in leptonic tau decay by the MAC collaboration gives a new world average[26] for the Michel ρ parameter for τ decay of 0.73 ± 0.07, to be compared with the 0.75 expected for a pure $V - A$ coupling of the W at the $\bar{\tau}\nu_\tau$ vertex. While much improved over the situation of a few years ago, one can exclude only $> 47\%$ $V + A$ at 95% confidence level.

The clean separation of τ events at PEP and PETRA has allowed the accurate measurement of the distribution of charged-prong multiplicity in its decay. The present world average numbers for the inclusive topological branching ratios[26] are $86.8 \pm 0.3\%$ for one-prong decays and $13.1 \pm 0.3\%$ for three-prong decays of the tau. The five -prong branching ratio is $\sim$ 0.14%, divided approximately equally between decays with and without extra neutrals.

The advent of vertex detectors has given us accurate measurements of the tau lifetime. Until this year the best measurements gave numbers near 0.29 picoseconds. With new measurements from ARGUS, CLEO, HRS, and MAC, this number has moved up somewhat to[26] 0.305 ± 0.009 picoseconds, with the error obtained from combining statistical and systematic errors in each measurement and

then averaging. For later reference we note that

$$\begin{aligned} \tau_\tau &= BR(\tau \to \nu_\tau e^- \bar{\nu}_e)\left(\frac{M_\mu}{M_\tau}\right)^5 \tau_\mu \\ &= BR(\tau \to \nu_\tau e^- \bar{\nu}_e)\ (1.595 \text{ picoseconds}). \end{aligned} \tag{37}$$

The present world average lifetime of the tau then corresponds to an electronic branching fraction of $19.1 \pm 0.6\%$, about 2σ from the direct measurement (see below).

- Leptonic Decays

Neglecting the mass of the electron, the width for the decay $\tau \to \nu_\tau e^- \bar{\nu}_e$ is

$$\Gamma(\tau \to \nu_\tau e^- \bar{\nu}_e) = \frac{G_F^2 M_\tau^5}{192\pi^3} = \frac{1}{1.595 \text{ picoseconds}} \tag{38}$$

Taking account of the mass of the muon, we have

$$\Gamma(\tau \to \nu_\tau \mu^- \bar{\nu}_\mu) = \frac{G_F^2 M_\tau^5}{192\pi^3}\ F(M_\mu/M_\tau), \tag{39}$$

where $F(M_\mu/M_\tau) = 0.97$. The present world average values for $\mathrm{BR}(\tau \to \nu_\tau e^- \bar{\nu}_e)$ and $\mathrm{BR}(\tau \to \nu_\tau \mu^- \bar{\nu}_\mu)$ among experiments where some have assumed, and others not, the factor of 0.97 between them, are[26] $17.9 \pm 0.4\%$ and $17.5 \pm 0.3\%$, respectively.

Note that leptonic decays like $\tau \to e\bar{e}e$, $\tau \to e\bar{\mu}e$, $\tau \to \mu\bar{e}e$, *etc.*, are forbidden in the standard model, as they involve lepton flavor changing neutral currents. The present upper limits on branching ratios for such processes have been reduced to the level of a few times 10^{-5} by the ARGUS collaboration.[27] As these are decays which involve only charged particles which must reconstruct to the beam

energy and the tau mass, the searches (up to now) have been straightforward ones which have turned up no candidates in the correct mass and energy bin. The limit essentially depends on the number of tau's produced, a very large sample of which BEPC should get for "free" when running above open charm (and therefore tau) threshold near the design luminosity.

- Semi-Hadronic Decays Through the Vector Current

We are now interested in decays of the form $\tau \rightarrow \nu_\tau + W^-_{\rm virtual}$, where the virtual W^- couples through a vector current to quarks, and thence to hadrons. Here we may make essential use the fact that the vector current in strangeness non-changing weak processes is an isospin rotation of the isovector part of the (vector) current of electromagnetism (*i.e.*, the conserved vector current hypothesis, CVC). There is consequentially a relation between the tau decay rate into ν_τ and a final hadronic state, f^-, and an integral over electron-positron annihilation cross sections for production of the corresponding hadronic final state, f^0. More precisely, the relation is:

$$\frac{\Gamma(\tau^- \rightarrow \nu_\tau f^-)}{\Gamma(\tau^- \rightarrow \nu_\tau e^- \bar{\nu}_e)} = \cos^2\theta_c \, \frac{3}{2\pi\alpha^2 M_\tau^8} \int_0^{M_\tau^2} dQ^2 Q^2 (M_\tau^2 - Q^2)^2 (M_\tau^2 + 2Q^2) \sigma_{e^+e^- \rightarrow f^0}(Q^2), \tag{40}$$

or

$$\frac{\Gamma(\tau^- \rightarrow \nu_\tau f^-)}{\Gamma(\tau^- \rightarrow \nu_\tau e^- \bar{\nu}_e)} = 2\cos^2\theta_c \int_0^1 dx (1-x)^2 (1+2x) \frac{\sigma_{e^+e^- \rightarrow f^0}}{\sigma_{pt}}, \tag{41}$$

in terms of the scaled variable $x = Q^2/M_\tau^2$ and the point cross section, $\sigma_{pt}(Q^2) = 4\pi\alpha^2/3Q^2$. As the vector, strangeness non-changing

current is even under G parity, the final state f contains an even number of pions.

The simplest and most important example of such a decay is $\tau^- \to \nu_\tau \pi^- \pi^0$. Here the strength of the weak vector current coupling to $\pi^- \pi^0$ can be related, using CVC, to that of the electromagnetic current to $\pi^+ \pi^-$.

The $\pi\pi$ system is very much dominated by the ρ resonance and an approximate result can be obtained[28] from computing $\tau^- \to \nu_\tau \rho^-$ in the narrow resonance approximation, with the coupling to the vector current extracted from $e^+ e^- \to \rho^0$ experiments. A more accurate result is obtained by integrating directly over the $e^+ e^- \to \pi\pi$ cross section using Eq. (41); one predicts[29]

$$\frac{\Gamma(\tau^- \to \nu_\tau \pi^- \pi^0)}{\Gamma(\tau^- \to \nu_\tau e^- \bar{\nu}_e)} = 1.23, \tag{42}$$

with an error which is due principally to the possible overall normalization error in the measurement of the $e^+ e^-$ cross sections. The agreement of Eq. (42) with experiment[26] provides a successful test of CVC.

A closely related result follows for the Cabibbo suppressed decay $\tau^- \to \nu_\tau (K\pi)^-$. Just as the $\pi\pi$ system is dominated by the ρ, we expect this decay to be dominated by the $K^*(890)$, as is indeed observed experimentally. The rate can be obtained from that for $\tau^- \to \nu_{/tau} \rho^-$ by multiplying by $\tan^2 \theta_c$ due to the strangeness-changing current, a factor to correct for phase space, and a correction for SU(3) breaking, yielding[30]

$$\frac{\Gamma(\tau^- \to \nu_\tau K^{*-})}{\Gamma(\tau^- \to \nu_\tau e^- \bar{\nu}_e)} = 0.064. \tag{43}$$

Because of the decay $K_s^0 \to \pi^+ \pi^-$, two ninths of these will appear

with as three-prong decays.

A more complicated situation is presented by $\tau^- \to \nu_\tau (4\pi)^-$. While this decay proceeds through the vector current and we can again relate the decay rate to an integral over e^+e^- cross sections, there are now two possible charge configurations in e^+e^- annihilation, $2\pi^-2\pi^+$ and $\pi^-\pi^+2\pi^0$, and two in τ decay as well, $\nu_\tau 2\pi^-\pi^+\pi^0$ and $\nu_\tau \pi^- 3\pi^0$. The constraint of being produced by different I_3 components of the same $I = 1$ weak current forces one linear relation between the rates for producing the respective charge states at each 4π invariant mass. As a result, not only can we write the $\tau^- \to \nu_\tau (4\pi)^-$ total decay rate as an integral over $\sigma_{e^+e^- \to 4\pi}$, but we have separately:

$$\frac{\Gamma(\tau^- \to \nu_\tau \pi^- 3\pi^0)}{\Gamma(\tau^- \to \nu_\tau e^- \bar{\nu}_e)} = \frac{3}{2\pi\,\alpha^2 M_\tau^8} \int_0^{M_\tau^2} dQ^2 Q^2 (M_\tau^2 - Q^2)^2 \times (M_\tau^2 + 2Q^2) \left[\frac{1}{2}\sigma_{e^+e^- \to 2\pi^-2\pi^+}(Q^2)\right] \tag{43a}$$

and

$$\frac{\Gamma(\tau^- \to \nu_\tau 2\pi^-\pi^+\pi^0)}{\Gamma(\tau^- \to \nu_\tau e^- \bar{\nu}_e)} = \frac{3}{2\pi\,\alpha^2 M_\tau^8} \int_0^{M_\tau^2} dQ^2 Q^2 (M_\tau^2 - Q^2)^2 (M_\tau^2 + 2Q^2) \times \left[\frac{1}{2}\sigma_{e^+e^- \to 2\pi^-2\pi^+}(Q^2) + \sigma_{e^+e^- \to \pi^+\pi^- 2\pi^0}(Q^2)\right] \tag{43b}$$

The e^+e^- cross sections are dominated by the ρ' resonance. Very rough results may be obtained by approximating the integrand using a single narrow resonance, but this is somewhat dangerous in that the mass ($\sim$ 1550 MeV) and width ($\sim$ 300 MeV) of the ρ' make

the factor $(M_\tau^2 - Q^2)^2(M_\tau^2 + 2Q^2)$ vary strongly over the resonance, considerably distorting its shape in τ decay.[30] Integrating directly over the e^+e^- cross sections gives:

$$\frac{\Gamma(\tau^- \to \nu_\tau \pi^- 3\pi^0)}{\Gamma(\tau^- \to \nu_\tau e^- \bar{\nu}_e)} = 0.055, \qquad (44a)$$

$$\frac{\Gamma(\tau^- \to \nu_\tau 2\pi^- \pi^+ \pi^0)}{\Gamma(\tau^- \to \nu_\tau e^- \bar{\nu}_e)} = 0.275, \qquad (44b)$$

and the sum,

$$\frac{\Gamma(\tau^- \to \nu_\tau (4\pi)^-)}{\Gamma(\tau^- \to \nu_\tau e^- \bar{\nu}_e)} = 0.33. \qquad (44c)$$

The result for the one charged-prong decay $\tau^- \to \nu_\tau \pi^- 3\pi^0$ in Eq. (44a) is rather certain as it depends only on the integral over the well measured cross section for $e^+e^- \to 2\pi^+ 2\pi^-$. The numerical result in Eq. (44b) is more uncertain because of the poorly measured cross section for $e^+e^- \to \pi^+\pi^- 2\pi^0$ above 1.4 GeV,
although it is in excellent accord with the direct measurement[26] of the branching ratio for this process in tau decay. Moreover, a subset of these decays arise from the process $\tau^- \to \nu_\tau \omega \pi^-$. This has been observed in tau decay,[31] permitting a test of CVC by comparing this data to that for $e^+e^- \to \omega\pi^0$ as a function of invariant $\omega\pi$ mass. CVC passes the test successfully.[31]

Decays involving more than four pions are very small, as is seen in particular for $\tau^- \to \nu_\tau (6\pi)^-$. In this case we can use the constraints that follow from the six pion system having total isospin one:

$$0 \le f_1 = \frac{\pi^- 5\pi^0}{\text{all } (6\pi)^-} \le 9/35 \ , \qquad (45a)$$

$$1/5 \leq f_3 = \frac{2\pi^-\pi^+3\pi^0}{\text{all}\,(6\pi)^-} \leq 4/5\ , \qquad (45b)$$

$$1/5 \leq f_5 = \frac{3\pi^-2\pi^+\pi^0}{\text{all}\,(6\pi)^-} \leq 4/5\ . \qquad (45c)$$

From Eq. (45c),

$$BR(\tau^- \to \nu_\tau(6\pi)^-) \leq 5BR(\tau^- \to \nu_\tau 3\pi^-2\pi^+\pi^0) \leq 0.005 \qquad (46)$$

and from Eqs. (45a) and (45c),

$$BR(\tau^- \to \nu_\tau\pi^-5\pi^0) \leq (9/7)BR(\tau^- \to \nu_\tau 3\pi^-2\pi^+\pi^0) \leq 0.001 \qquad (47)$$

Nor can decays involving eta mesons be appreciable. The simplest example proceeding through the vector current in the standard model is $\tau \to \nu_\tau\eta 2\pi$. Only within the past year have data for $\sigma_{e^+e^-\to\eta\pi^+\pi^-}$ been published which cover the full energy region needed for performing the integral in Eq. (41). The cross sections are at most a few nanobarns, and carrying out the calculation[32] gives a branching ratio for $\tau^- \to \nu_\tau\eta\pi^-\pi^0$ of 0.15%. Even taking 5 nb as a generous upper limit on the $e^+e^- \to \eta\pi^+\pi^-$ cross section above 1.4 GeV produces an upper limit of 0.24%.

- Semi-Hadronic Decays Through the Axial-Vector Current

The simplest decay that proceeds through the axial-vector current is $\tau^- \to \nu_\tau\pi^-$, which can be precisely calculated because the strength of the pion's coupling to the axial-vector current is directly

determined in the leptonic decay of the pion. Exactly the same quantity, $f_\pi \cos\theta_c$, is relevant in $\tau^- \to \nu_\tau \pi^-$:

$$\frac{\Gamma(\tau^- \to \nu_\tau \pi^-)}{\Gamma(\tau^- \to \nu_\tau e^- \bar{\nu}_e)} = \frac{(f_\pi \cos\theta_c)^2}{M_\tau^2} 12\pi^2 \left[1 - \frac{m_\pi^2}{M_\tau^2}\right]^2 = 0.607 \ . \qquad (48)$$

The related, Cabibbo suppressed decay, $\tau^- \to \nu_\tau K^-$, also has the quantity of relevance, $f_K \sin\theta_c$, directly measured elsewhere (in the dominant decay of the charged kaon), yielding

$$\frac{\Gamma(\tau^- \to \nu_\tau K^-)}{\Gamma(\tau^- \to \nu_\tau e^- \bar{\nu}_e)} = \frac{(f_K \sin\theta_c)^2}{M_\tau^2} 12\pi^2 \left[1 - \frac{m_K^2}{M_\tau^2}\right]^2 = 0.0395 \ . \qquad (49)$$

The decay $\tau \to \nu_\tau (3\pi)^-$ can not be calculated with great accuracy, although it was expected[28] to be dominated by the A_1 resonance with a branching ratio of order 10%. Excellent measurements of the decay $\tau^- \to \nu_\tau 2\pi^- \pi^+$ now exist with a branching ratio[26] of $6.6 \pm 0.4\%$ and showing a clear A_1 resonance in the $J^P = 1^+$ partial wave, decaying almost entirely through $\pi\rho$.

Measurements of the other charge configuration, $\tau^- \to \nu_\tau \pi^- 2\pi^0$ are not nearly so good.[26] We may gain information on it, however, from the constraint of having total isospin one for the $(3\pi)^-$ system; it follow that independent of the dynamics

$$1/5 \leq f_1 = \frac{\pi^- 2\pi^0}{\text{all } (3\pi)^-} \leq 1/2 \ , \qquad (50a)$$

and

$$1/2 \leq f_3 = \frac{2\pi^- \pi^+}{\text{all } (3\pi)^-} \leq 4/5. \qquad (50b)$$

Thus the number of three-prong tau decays must be greater than that of one-prong decays for $\tau^- \to \nu_\tau (3\pi)^-$. The equality of the two

charge configurations occurs when two of the pions are in an isospin one state, *i. e.*, precisely the case of relevance where the quasi-two body $\pi\rho$ channel dominates. The branching ratio for $\tau^- \to \nu_\tau \pi^- 2\pi^0$ is, if anything, measured[26] to be slightly bigger than that for $\tau^- \to \nu_\tau 2\pi^-\pi^+$, but is consistent with equality within the statistical and especially the systematic errors of background subtractions.

Other decays through the axial-vector current are measured to be small, like the Cabibbo suppressed decay $\tau \to \nu_\tau (K\pi\pi)^-$, or can be bounded, like $\tau^- \to \nu_\tau (5\pi)^-$, from the very small number of five-prong decays using isospin.[30]

- The "Missing" One-Prongs

Having done all the work of enumerating the decay modes of the tau in the standard model, we come to the one outstanding problem. We have discussed the decays $\tau \to \nu_\tau e\bar{\nu}_e$, $\tau \to \nu_\tau \mu\bar{\nu}_\mu$, $\tau \to \nu_\tau \pi$, $\tau \to \nu_\tau 2\pi$, $\tau \to \nu_\tau 3\pi$, and $\tau \to \nu_\tau 4\pi$, plus a number of smaller modes. They occur at the expected rates[26,30] and the sum of their exclusive branching ratios accounts for almost 90% of tau decays. However, there are no modes thought to be of consequence which haven't been included and there is a nagging problem in accounting for all tau decays.[26,30,32] In particular, it is difficult to account for all the one-prong decays of the tau.

In more detail, the problem arises as follows. Consider first three-prong decays, which are shown in Table I. All the theoretical calculations of decay branching ratios are taken from the discussion above and are normalized to that for $\tau \to \nu_\tau e\bar{\nu}_e$, for which we take the world average value of 17.9%. Where theory and experiment can be compared, they are in excellent agreement. Moreover, the sum of all

the exclusive decays measurements is in agreement with the inclusive three-prong branching ratio.

The agreement between theory (where there is a prediction of some accuracy) and experiment (where there is a definite measurement) is also very good in the case of tau decays involving one charged prong, as shown in Table II. Note in particular that aside from the leptonic decays (whose branching ratio is used as an input), the excellent agreement between theory and experiment for the semi-hadronic decays $\tau \to \nu_\tau \pi$, $\tau \to \nu_\tau K$, and $\tau^- \to \nu_\tau \pi^- \pi^0$.

The theoretical upper bound on the branching ratio for $\tau^- \to \nu_\tau \pi^- 2\pi^0$ comes from Eq. (50) and the measured rate for $\tau^- \to \nu_\tau 2\pi^- \pi^+$ in Table I. Adding one percent for the sum of small modes not explicitly written in Table II, the sum of the one-prong branching ratios from theory is $< 80\%$, to be compared with the $86.8 \pm 0.3\%$ inclusive one-prong branching ratio measured experimentally. We have accounted for all the purely leptonic modes and all the modes of the form $\tau^- \to \nu_\tau (n\pi)^-$ of any substance, as well as Cabibbo suppressed modes. Where are the remaining of one-prong decays?

There is no reason to suspect that they come from the decays in Table II for which there are no experimental numbers entered. The only two expected to be substantial are $\tau^- \to \nu_\tau \pi^- 2\pi^0$ and $\tau^- \to \nu_\tau \pi^- 3\pi^0$. The former should occur at the same rate ($6.6 \pm 0.4\%$) as $\tau^- \to \nu_\tau 2\pi^- \pi^+$ (see above). The latter is predicted theoretically on the basis of CVC and well measured e^+e^- cross sections; it should be solid. Adding these theoretical branching ratios (and that for $\tau \to \nu_\tau \eta \pi^- \pi^0$) to the second column of Table II gives a sum of $78 \pm 2\%$ for the branching ratios of the exclusive channels. Although with bigger experimental error bars, this is the situation that was already

TABLE I

THREE CHARGED PRONG DECAYS OF THE TAU

Decay Mode	Branching Ratio (%) Theory	Experiment[26]
$\tau^- \to \nu_\tau 2\pi^-\pi^+$		6.6 ± 0.4
$\tau^- \to \nu_\tau 2\pi^-\pi^+\pi^0$	4.9	5.2 ± 0.5
$\tau^- \to \nu_\tau (K\pi)^-$	0.3	0.3 ± 0.1
$\tau^- \to \nu_\tau K^-\pi^-\pi^+(\pi^0)$		0.22 ± 0.14
$\tau^- \to \nu_\tau K^-K^+\pi^-$		0.22 ± 0.14
$\tau^- \to \nu_\tau 2\pi^-\pi^+3\pi^0$	< 0.4	
TOTAL EXCLUSIVE		12.5 ± 0.7
TOTAL INCLUSIVE		13.1 ± 0.3

TABLE II

ONE CHARGED PRONG DECAYS OF THE TAU

Decay Mode	Branching Ratio (%) Theory	Experiment[26]
$\tau^- \to \nu_\tau e^-\bar{\nu}_e$	17.9 (Input)	17.9 ± 0.4
$\tau^- \to \nu_\tau \mu^-\bar{\nu}_\mu$	17.4	17.5 ± 0.3
$\tau^- \to \nu_\tau \pi^-$	10.9	10.9 ± 0.6
$\tau^- \to \nu_\tau \pi^-\pi^0$	22.0	22.1 ± 1.1
$\tau^- \to \nu_\tau \pi^- 2\pi^0$	≤ 7.0	
$\tau^- \to \nu_\tau \pi^- 3\pi^0$	1.0	
$\tau^- \to \nu_\tau \pi^- 4\pi^0$	< 0.1	
$\tau^- \to \nu_\tau \pi^- 5\pi^0$	< 0.1	
$\tau^- \to \nu_\tau (K\overline{K})^-$		< 0.26
$\tau^- \to \nu_\tau (K\overline{K}\pi)^-$	< 0.5	
$\tau^- \to \nu_\tau \eta\pi^-\pi^0$	0.15	
$\tau^- \to \nu_\tau K^-$	0.7	0.7 ± 0.2
$\tau^- \to \nu_\tau (K\pi)^-$	0.9	1.1 ± 0.3
TOTAL EXCLUSIVE	< 80	
TOTAL INCLUSIVE		86.8 ± 0.3

noted over two years ago.[30]

A sharpening of the problem has come from the increased accuracy with which many of the main branching ratios are known and from measurements of the branching ratio for $\tau \to \pi^- +$multineutrals, which includes $\tau^- \to \nu_\tau \pi^- 2\pi^0$, $\tau^- \to \nu_\tau \pi^- 3\pi^0$, $\tau^- \to \nu_\tau \eta \pi^- \pi^0$), *etc.* This measurement gives consistently higher values[33] than is expected theoretically from the sum of the components. (It is difficult to reconstruct the individual multi-neutral decay modes.) For a time it was suspected that modes involving eta's were the "missing" modes,[34] but this was recently shown to be untenable[32] in the standard model.

In the past few months, the HRS collaboration claimed that there were decays involving the eta at the 5% level in exactly the mode, $\tau^- \to \nu_\tau \pi^- \eta$, that is not expected in the standard model.[35] (The $\eta\pi$ system, which is G odd, has natural spin-parity and in the standard model it must come from the vector current, which is G even; we have by definition a process that involves a second class current.) Within the standard model this should happen at a level of roughly α^2 in the rate when compared to processes arising through the usual first class currents and such a decay would be completely negligible.[36] Other experiments have since contradicted this result.[37]

With other conventional (or even unconventional) modes that contribute to one-prong tau decays severely limited, there are two possible ways out of the problem. The first is that the branching ratio for $\tau \to \nu_\tau e \bar{\nu}_e$, which we took to be 17.9% (and to which we normalized all our theoretical predictions), should be $\approx$ 19%. This would scale up all the predicted branching ratios by $\approx 6\%$ and make the sum for theory agree with the measurement of the one-prong inclusive branching ratio. Of course it is one thing to scale up the

theory by a common factor, as all the predictions are normalized to the single mode $\tau^- \to \nu_\tau e^- \bar{\nu}_e$, and another to get all the individually measured experimental branching ratios to change, all in the same direction! Nevertheless this is what the present world average value of the tau lifetime indicates (by 2σ) is the solution, and it is the easiest (purely from the point of view of not straining the standard model) way out.

Second, there is the possibility of something new. This is the direction in which the directly measured branching ratios, and particularly that for $\tau \to \pi^- +$ multineutrals, points. But what? It is hard to find a scenario for this situation which is not very contrived (especially if it is not to be in conflict with other existing experiments).

The experiments necessary to decide between these two possibilities are hard as well. I suspect that although the puzzle has been sharpened considerably in the past year, it will take some additional measurements over the next several years by detectors well-instrumented for detection of neutrals to resolve it.

5. HEAVY QUARK SPECTROSCOPY

The spectroscopy of heavy quark systems is the showcase of our understanding of hadron physics. It is sometimes even advertised as the "hydrogen atom of strong interactions".

We do indeed have a fundamental gauge theory of the strong interactions in Quantum Chromodynamics (QCD). This theory in principle explains the vast body of data that has been accumulated over the past dozen years.[38] However, as we will soon see, the connection between the fundamental theory and experimental observables

is not (yet) as it is for the electroweak gauge theory, $SU(2) \times U(1)$. The situation we confront is essentially non-perturbative, and the underlying gauge theory is one-step-removed from detailed numerical confrontation with experiment.

What we have at present to accompany the data is more like a phenomenology, inspired or backed-up by QCD. At times it gives us an asymptotic form. At other times it gives an expression for the general structure of some quantity, with free parameters or hadronic matrix elements contained within it. While these latter are determined by QCD in principle, for the moment they are often only approximately calculable (at best). So we take a peek at the data and 'adjust' the parameters, thereby learning something about the nature of the solution of QCD. Then we predict additional quantities and iterate the whole process again.

This is then a place where theory and experiment intertwine; basic theory, models inspired by theory, and experiment meet and influence one another. It is quite different from the situation in the electroweak theory where there is a well-defined and clean set of perturbative predictions to compare with experiment. In one sense this is frustrating, as one would like clean and decisive tests of the underlying theory. In another sense, this is what makes it exciting and makes the subject still worth pursuing: the interplay between theory and experiment is interesting in itself, and we often learn things which are applicable either as techniques or as results in other areas as well.

In fact, progress has been made and continues to be made.[39] Eventually, one has every reason to believe that we will be able to calculate the "potential" from first principles, presumably using lattice

techniques. Everything then will be predicted starting from the QCD Lagrangian. We have come a long way in this direction already,[40] and perhaps in a Charm Symposium of a few(?) years hence we may well no longer need to give such a talk on this subject.

- The Spin Independent Potential

Let's start with the nonrelativistic, spin independent potential. Even the use of the word potential is a bit loose for we are starting with a strong interaction bound state problem and extracting from it an effective two-body, non-relativistic potential. The problem at hand is intrinsically a relativistic field-theoretic one in which the $q\bar{q}$ sector, for example, is coupled to what happens in the $qq\bar{q}\bar{q}$, $q\bar{q}$ + gluon, *etc.*, sectors as well. Some justification for the success of the "naive," non-relativistic approach have recently been given,[41] but simultaneously questions have been raised as to the effect of what is being neglected, and how it changes the relationship between parameters in the underlying theory and the effective potential.[42] There is even a whole, well-developed approach to understanding some of the same body of data through QCD sum rules.[43]

With these questions in mind, we shall proceed to think in terms of a two-body potential obtained by expanding in powers of v^2/c^2. Indeed, such an expansion does make some sense, for the smallness of v^2/c^2 in a system composed of a heavy quark and heavy antiquark encourages us to think in terms of a non-relativistic potential with spin-dependent terms which arise first in order v^2/c^2 and give rise to splittings which are smaller than those between levels of the spin independent potential. In the cases at hand v^2/c^2 is ~ 0.4 for the low-lying charmonium states and $\lesssim 0.1$ for the low-lying bottomonium

states. Still, when we go to compare with the calculated energy levels with experiment we need to bear in mind that predictions from alternate potentials that differ by 10 or 20 MeV are not necessarily significant in favoring one potential over another. We may in any case be making (especially for charmonium) approximations to the exact theory in "deriving" a non-relativistic potential which render the resulting model incapable of discriminating differences at this level.

We have good theoretical guidance in two opposite regimes. At short distances, or equivalently large momentum scales, there is the property of asymptotic freedom. The running coupling becomes smaller as we decrease the distance scale at which we work, and the effective potential approaches the lowest order one gluon exchange result,

$$V(r) \to -\frac{4}{3}\frac{\alpha_s}{r} \tag{51}$$

as $r \to 0$.

Note the additional factor of $\frac{4}{3}$ compared to the usual Coulomb interaction; this arises from color. It is so pervasive that it is worth a short derivation, so here it is again.[44] We want the additional factor due to color. It arises from a normalized color singlet quark-antiquark wave function, $\delta_{ij}/\sqrt{3}$ in the initial and final state, a color SU(3) matrix $\lambda^a_{ij}/2$ at each quark-gluon vertex, and a color sum over the (eight) gluons, δ^{ab}, in the gluon propagator. The sum over indices gives a trace:

$$\sum_{a,b=1}^{8}\sum_{i,j,k,l=1}^{3}\frac{\delta_{il}}{\sqrt{3}}\frac{\lambda^a_{ij}}{2}\frac{\delta_{jk}}{\sqrt{3}}\frac{\lambda^b_{kl}}{2}\delta^{ab} = \frac{1}{3}\sum_{a=1}^{8}Tr\left[\frac{\lambda^a}{2}\frac{\lambda^a}{2}\right] = \frac{1}{3}(8)\frac{1}{2} = \frac{4}{3}. \tag{52}$$

The trace of $\frac{\lambda^a}{2}\frac{\lambda^a}{2}$ is just $\frac{1}{2}$, as befits the generators of a Lie algebra (or, as may be checked for the case of the λ matrices of $SU(3)$ directly); thus the ubiquitous factor of $4/3$.

That's one regime. The second regime where we have very solid theoretical input is at the other extreme, as $r \to \infty$, and we have confinement of the quarks. From relatively general theoretical arguments we know that the potential behaves as a linear function of the distance:

$$V(r) \to kr. \tag{53}$$

There is a corresponding physical picture of a "color-electric flux tube" joining the quarks. As you pull the quarks apart, the flux tube is increased in length, at the cost of an increase in energy per unit length given by the constant k. The value of k is about 0.2 GeV^2.

Given those two regimes we might hope to construct the full potential. The simplest possibility is to simply add together terms with the correct functional dependence in the two asymptotic regimes. This is basically the Cornell potential,[45]

$$V(r) = \frac{-0.48}{r} + \frac{r}{(2.34\ \text{GeV}^{-1})^2}, \tag{54}$$

with the two coefficients having been adjusted to fit the charmonium spectrum, although the model does a quite adequate job in describing bottomonium as well.

In the late 70's Richardson combined the two behaviors in one form.[46] Here is his potential in configuration space,

$$V(r) = \frac{8\pi}{33 - 2n_f}\,\Lambda\left(\Lambda r - \frac{f(\Lambda r)}{\Lambda r}\right), \tag{55}$$

with

$$f(t) = 1 - 4\int_1^\infty \frac{dq}{q}\ \frac{e^{-qt}}{\ell n^2(q^2-1)+\pi^2}, \tag{56}$$

where it looks like two terms. What's going on is more transparent in momentum space where it can be written as one term:

$$\widetilde{V}(q^2) = -\frac{4}{3}\ \frac{12\pi}{33-2n_f}\ \frac{1}{q^2\ell n(1+q^2/\Lambda^2)}. \tag{57}$$

As q^2 goes to infinity, this expression becomes precisely $\frac{4}{3}\alpha_s/q^2$, as required from one gluon exchange. In the other limit of $q^2 \to 0$, one obtains something proportional to $1/q^4$. This may be an unfamiliar behavior in momentum space, but if you Fourier transform back to configuration space, this is just a potential which is linear in r. It is by no means guaranteed that you will get the "right" coefficient to fit the data. Richardson, along with others[47] who proposed modified versions of this potential, showed that you do in fact get a very reasonable, even excellent, description of the data, especially for bottomonium.

Finally, Martin has proposed the potential[48]

$$V(r) = (5.82\ \text{GeV})\ \left(\frac{r}{1\ \text{GeV}^{-1}}\right)^{0.104}. \tag{58}$$

This potential, with the absurd power of 0.104, lacks fundamental motivation (as Martin knew very well). We will use it as a kind of straw man, for it also does quite a credible job of fitting the charmonium and bottomonium data. But why?

The reason can be seen in Figure 4. Here you can see the various potentials for comparison purposes. In particular, aside from

being displaced vertically from one another a little bit (which you are free to remove by adjusting the quark mass), they all have about the same behavior between 0.1 and 1 fermi. This can be seen even better looking at the inset, where r is given on a logarithmic scale and the potentials have been shifted slightly relative to one another vertically, as discussed above. Also shown are the mean radii of the psi, upsilon, *etc.* These are all between 0.1 and 1 fermi, and that's why the different potentials all can fit the data; the wave functions for these states mostly (but not entirely) live in this region where the potentials coincide.

Thus, where our theoretical insight is best and tells us something very well-defined for the behavior of the spin independent potential, it is mostly irrelevant to the present data. Conversely, the experiments up to now mostly tell us about a region where theory does not have much to say about the spin independent potential. In fact, one can invert the data to obtain a potential[49] which describes what happens from 0.1 to 1 fermi. Within errors, it coincides with what we have just seen in Figure 4.

Even without a particular potential and detailed calculation, we can get a good qualitative idea of what the spectrum of states will look like. In Figure 5a is the familiar spectrum due to a Coulomb potential, which is what we have at short distances. The ground state with $\ell = 0$ is labelled 1S; its radial excitation (labelled 2S) is degenerate in the case of a Coulomb potential with the first set of $\ell = 1$ states (labelled 1P), and so on. As an example of a confining potential which we want at large distance, Figure 5b shows the levels of a three dimensional harmonic oscillator, which is more familiar than a linear potential and turns out also to be a special "boundary"

case from the point of view of the ordering of levels. What will happen when we combine the two? For the energy levels we will naturally get something in between Figures 5a and 5b. This is shown in Figure 5c. The ordering, starting at the bottom, is 1S, 1P (between the 1S and 2S as for the harmonic oscillator, but closer to the 2S, as it would be degenerate with it for the Coulomb potential), 2S, 1D (above 2S as for Coulomb, but close to it, as it would be degenerate for the harmonic oscillator), *etc.* You can therefore get a qualitative understanding of the spectrum from quite general considerations.

There is a theorem[50] which is quite useful in this regard and puts the qualitative ordering discussed above on a rigorous footing. It states that if $\bigtriangledown^2 V(r) > 0$ for all r, something which is true for all suggested potentials, then $E_{nS} > E_{(n-1)P}$. Related theorems are provable for the ordering of levels with other angular momenta.[51]

Each of the potentials discussed above can give a quantitative understanding of the levels of charmonium (Figure 1) and bottomonium (Figure 2) to 30 MeV or better. Even the statement that one flavor independent potential can fit both systems is nontrivial. The agreement between theory and experiment, which is shown in Schindler's lectures,[38] I regard as quite spectacular. It includes not just energy levels, but wave functions at the origin for the nS states as well. Where there is a disagreement, it is difficult to know whether to blame it on the potential or on corrections due to relativistic or other effects which have been left out.

When and how will we be able to distinguish between potentials? The answer appears to be that toponium will provide the crucial system. In Figure 6 is shown the spectrum of toponium[52] corresponding to m_t in the range of 40 to 50 GeV. There are 10 or more nS states

below open top threshold; near that threshold there is one state per 100 MeV.

More important for the physics at hand, aspects of the spectrum of states and of the wave functions at the origin are now sensitive to the behavior of the potential at short distances. The values of the wave function at the origin are shown in Figure 7, with that for the ground state corresponding to a width into electron-positron pairs, which is proportional to the square of the wave function at the origin, of about 9 keV (from the one photon intermediate state alone). This is larger than one would expect from a naive extrapolation from the psi and the upsilon by about a factor of two. We are beginning to see the effect of the $1/r$ term in the potential pulling in the wave function. Higher levels are affected less, as seen in Figure 7, for on average they live at larger distances.

The same physical effect is shown in Table III, with the t quark mass assumed to be 50 GeV. Notice in particular how much the energy of the 1S level is pulled down by the Cornell potential (3 GeV below 2 m_t). This is to be compared with 1.7 GeV for the Richardson and 1.4 GeV for the Martin potentials. Correspondingly the radius of the 1S state is much smaller for the Cornell potential and the 2S to 1S difference much bigger. Even more dramatic is the comparison of the wave function at the origin for the 1S state, where the Cornell result is about 3 times that for Richardson and 9 times that for Martin. Remember, the predicted electron-positron width goes like these numbers squared!

Before leaving this subject, we should note that this same property makes toponium a fairly sensitive place to look for extra short range forces. A good example is the presence of an extra term in the

TABLE III

CHARACTERISTICS OF TOPONIUM STATES

FOR VARIOUS POTENTIALS

Potential	E_{1S} (GeV)	$< r_{1S} >$ (fermi)	$E_{2S} - E_{1S}$ (GeV)	$\Psi(0)_{1S}$ (GeV$^{3/2}$)
"Cornell"	97.1	0.028	2.2	23.3
"Richardson"	98.3	0.048	1.0	8.5
"Martin"	98.6	0.084	0.5	2.7

potential due to neutral Higgs exchange with enhanced couplings.[53] This changes both the wave functions and the ordering of the energy levels in a characteristic fashion, and allows it to be distinguished from a simple change in the strength of the $1/r$ piece of the strong interaction potential.

- The Spin Dependent Potential

Now we turn to the spin dependent potential. In its full glory it has the form:

$$\begin{aligned} V_{SD}(r) = & \left(\frac{\vec{S}_1 \cdot \vec{L}}{2m_1^2} + \frac{\vec{S}_2 \cdot \vec{L}}{2m_2^2} \right) \left(\frac{dV(r)}{rdr} + 2\frac{dV_1(r)}{rdr} \right) \\ & + \frac{(\vec{S}_1 + \vec{S}_2) \cdot \vec{L}}{m_1 m_2} \frac{dV_2(r)}{rdr} \\ & + \frac{1}{6m_1 m_2} \left(6\vec{S}_1 \cdot \hat{r}\vec{S}_2 \cdot \hat{r} - 2\vec{S}_1 \cdot \vec{S}_2 \right) V_3(r) \\ & + \frac{2}{3m_1 m_2} \vec{S}_1 \cdot \vec{S}_2 \, V_4(r) \end{aligned} \tag{59}$$

as given by Eichten and Feinberg[54] and discussed pedagogically by

Eichten[55] and by Peskin.[56] The term $V(r)$ is the spin independent potential we discussed previously. The other terms involving V_1, V_2, V_3, and V_4 are not necessarily simply related to $V(r)$. As can be seen particularly clearly in Michael Peskin's lectures,[56] these extra terms originate in expectation values of color electric and magnet fields which are different than those that enter in the spin independent potential; they are new objects.

Although the situation is more complicated than one might have hoped, at least initially it was possible to entertain the idea that all the new spin dependent terms are of short range. This hope was dashed when it was shown that[57]

$$V(r) + V_1(r) = V_2(r). \tag{60}$$

Since V has a long range confining part, so must either V_1 or V_2.

Let us use Eq. (60) to eliminate V_1 from the spin dependent potential. It now reads:

$$\begin{aligned} V_{SD}(r) = & \left(\frac{\vec{S}_1 \cdot \vec{L}}{2m_1^2} + \frac{\vec{S}_2 \cdot \vec{L}}{2m_2^2} \right) \left(\frac{-dV(r)}{rdr} + 2\frac{dV_2(r)}{rdr} \right) \\ & + \frac{(\vec{S}_1 + \vec{S}_2) \cdot \vec{L}}{m_1 m_2} \frac{dV_2(r)}{rdr} \\ & + \frac{1}{6m_1 m_2} \left(6\vec{S}_1 \cdot \hat{r}\vec{S}_2 \cdot \hat{r} - 2\vec{S}_1 \cdot \vec{S}_2 \right) V_3(r) \\ & + \frac{2}{3m_1 m_2} \vec{S}_1 \cdot \vec{S}_2 \, V_4(r). \end{aligned} \tag{61}$$

Could it now be that the remaining new potentials V_2, V_3, and V_4 are short range?

Not only is there no information to contradict this possibility, but it is supported by the results of recent lattice gauge theory calculations,[58,59] the results of some of which[22] are shown in Figures 8, 9, 10, and 11. We see that V_1 (which we have eliminated from Eq. (61)) is not short range, but V_2 looks completely different; it is very short range, and similarly for V_3 and V_4. All of this is done on a $16^3 \times 32$ lattice. It should be regarded as a qualitative result, but an important step toward the more quantitative results we can expect in the future.

Let us now go back to the spin dependent potential in the equal mass case relevant to quarkonium. We rewrite it a little bit, combining the first two terms:

$$\begin{aligned} V_{SD}(r) = \frac{\vec{S}\cdot\vec{L}}{2m^2}\left(\frac{-dV(r)}{rdr} + 4\frac{dV_2(r)}{rdr}\right) \\ + \frac{1}{12m^2}\left(6\vec{S}\cdot\hat{r}\vec{S}\cdot\hat{r} - 2\vec{S}\cdot\vec{S}\right)\ V_3(r) \\ + \frac{1}{6m^2}\left(2\ \vec{S}\cdot\vec{S} - 3\right)\ V_4(r). \end{aligned} \tag{62}$$

Now, to get a simple physical picture of what is happening, let us forget for a moment the previous discussion about the spin dependent and spin independent potentials being independent entities. Let us consider what we would obtain from a (relativistic) four-fermion interaction arising from the exchange of a vector and a scalar between a quark and the antiquark of equal mass. In momentum space this is represented by an interaction:

$$L_{int} = \tilde{s}(q^2)\ \bar{u}u\bar{v}v + \tilde{v}(q^2)\ \bar{u}\gamma_\mu u\bar{v}\gamma^\mu v. \tag{63}$$

If we do an expansion in powers of v^2/c^2, the static limit is the spin

independent potential $v + s$, and the spin dependent terms give the Breit-Fermi potential, which in configuration space is:

$$V_{SD}(r) = \frac{\vec{S}\cdot\vec{L}}{2m^2}\left(-\frac{dv(r)+ds(r)}{rdr}+4\frac{dv(r)}{rdr}\right)$$
$$+\frac{1}{12m^2}\left(6\vec{S}\cdot\hat{r}\vec{S}\cdot\hat{r}-2\vec{S}\cdot\vec{S}\right)\left(\frac{dv(r)}{rdr}-\frac{d^2v(r)}{d^2r}\right) \qquad (64)$$
$$+\frac{1}{6m^2}\left(2\ \vec{S}\cdot\vec{S}-3\right)\ \bigtriangledown^2 v(r).$$

The term $-(dv(r)+ds(r))/rdr$ in the first line is due to the familiar Thomas precession, and it is followed by usual spin-orbit, tensor (on the second line), and spin-spin (on the third line) interactions, each with a coefficient related to $v(r)$ or $s(r)$.

Now we are in a position to compare what is in Eq. (64) to the generic decomposition in Eq. (62) involving V_1, V_2, and V_3. First, the spin independent potential V is here given by the sum of the vector and scalar potentials, $v+s$. Second, the spin dependent potentials V_2. V_3, and V_4 are all expressible in terms of derivatives of only the vector part of the potential, v. Hence, if v is related to gluon exchange and its associated $1/r$ behavior, then the potentials V_2, V_3, and V_4 are all short range in character.

This encourages us to make the following division: the scalar term is long range and associated with quark confinement, while the vector term is short range (we include $1/r$ behavior as short range) and associated with gluon exchange. From the short range Coulomb-like piece one obtains the spin dependent terms we are long accustomed to in atomic physics: a spin-orbit interaction (minus the piece due to Thomas precession), a tensor interaction, and a spin-spin interaction. As you go to long range, the confining interaction, which

is Lorentz scalar in character, becomes dominant. The associated physical picture[60] has a color flux tube that connects the quark and antiquark, and as they rotate around each other the flux tube rotates along with them. Consequently there are no spin dependent forces generated from this part of the potential, aside from the Thomas term which comes in with a minus sign and is generated from the spin rotation associated with Lorentz transforming from the center-of-mass to the quark or antiquark rest frame. So we get a simple way of understanding all the terms in Eq. (64). From now on we will take this identification of v and s seriously. Occasionally we will slip over to the stronger assumption that $s(r) \propto r$ and $v(r) \propto 1/r$, even to the point of thinking that we know the respective constants of proportionality.

- The Spin-Spin Interaction

The spin-spin interaction, which in the equal mass case takes the form

$$V_{SS} = \frac{1}{6m^2} \left(2\ \vec{S}\cdot\vec{S} - 3\right)\ \bigtriangledown^2\, v(r), \tag{65}$$

is the analogue for the color forces of QCD of the interaction which gives rise to the hyperfine splittings between atomic levels. If we are brave enough to follow this analogy further and insert a $1/r$ behavior for $v(r)$, then since $\bigtriangledown^2(1/r) = -4\pi\delta^3(\vec{r})$, the spin-spin interaction is of very short range!

This delta function at the origin can be tested by noting that for quarkonium p-wave states, whose wave function at the origin vanishes, the expectation value of the spin-spin interaction should be zero. Therefore the center-of-gravity of the three states with total quark spin one and $J = 0$, 1, and 2 should be the same as the mass

of the $J = 1$ state with quark spin zero:

$$\frac{5M_2 + 3M_1 + M_0}{9} = M_{\text{spin singlet}}. \tag{66}$$

(The p-wave states with total quark spin one are split in mass by the spin-orbit and tensor interactions, and the weighted average is just such as to cancel out these contributions).

For charmonium, the left-hand side of Eq. (66) is 3525.38 MeV, and an experiment in the last days of the ISR found a few candidate events with an average mass of 3525.4 ± 0.8 MeV.[61] For the bottomonium system, the corresponding values for the center-of-gravity are 9900.2 MeV for the 1P states and 10,261.6 MeV for the 2P states.[38] It would be very interesting to measure the mass of the corresponding singlet p wave states for bottomonium. There is a little bit of evidence from the CLEO experiment, studying $\pi\pi$ transitions from the 3S resonance, for a state a little below the 1P center-of-gravity.[62] As the $\bar{b}b$ system is more non-relativistic than $\bar{c}c$, the agreement with Eq. (66) should be excellent. Otherwise, the agreement in the charm case was an accident, and we had better take a close look at our assumptions on the short range nature of the spin-spin interaction.

Let us specialize to a system that consists of one heavy and one light quark. The assumption that $v(r)$ behaves as $1/r$ still gives a delta function at the origin in the part of the potential that gives the spin-spin interaction. Furthermore, the physical origin of this term in a quark color magnetic moment interacting with an antiquark color magnetic moment is still correct, and so it still depends inversely on the product of the quark mass and the antiquark mass (see the coefficient of V_4 in Eq. (59)). For example, the mass difference of the

ground state vector and pseudoscalar states should behave as

$$M(^3S_1) - M(^1S_0) \propto \frac{|\Psi(0)|^2}{m_i m_j}. \tag{67}$$

If we use the fact that the spin-spin splitting is small and that in terms of constituent masses,

$$M(^3S_1) \sim M(^1S_0) \sim m_i + m_j, \tag{68}$$

then we can rewrite Eq. (17) in terms of mass squared,

$$M^2(^3S_1) - M^2(^1S_0) \propto \frac{m_i + m_j}{m_i m_j}|\Psi(0)|^2 \propto |\Psi(0)|^2/\mu_{ij} \tag{69}$$

and get a result that depends on the reduced mass of the quark-antiquark system.

One the other hand, in a system composed of a heavy and a light quark we have a atomic hydrogen-like situation with the heavy quark playing the role of the nucleus and the light quark primarily living at "large" distances. The corresponding wave function is determined by the long distance part of the potential which behaves as kr. However, for a potential which behaves as r^β, the Schrodinger equation yields a scaling law that makes[63]

$$|\Psi(0)|^2 \propto \mu_{ij}^{\frac{3}{2+\beta}}.$$

Therefore, corresponding to the case at hand with $\beta = 1$,

$$|\Psi(0)|^2 \propto \mu_{ij},$$

and substituting this into Eq. (69), one finds[64,65]

$$M^2(^3S_1) - M^2(^1S_0) \sim \text{const.} \tag{70}$$

This relation is compared to experiment in Table IV. The input

masses come from the Particle Data Tables[66] except for the $F - F^*$ mass splitting where the new result from the Mark III experiment is used.[67]

TABLE IV

GROUND STATE VECTOR – PSEUDOSCALAR MASS^2 DIFFERENCES

Mass^2 Difference	Experimental value[66,67] in GeV^2
$M_\rho^2 - M_\pi^2$	0.57
$M_{K^*}^2 - M_K^2$	0.56
$M_{D^*}^2 - M_D^2$	0.55
$M_{F^*}^2 - M_F^2$	0.55
$M_{B^*}^2 - M_B^2$	0.55

The $\rho - \pi$ difference is thrown in for good measure, even though it involves only light quarks. Even the $K^* - K$ case should not be in Table IV, for the strange quark is not all that heavy. Of course, they are in Table IV because they all agree magnificently with each other, so much the more so now that we have the new data on the $F^* - F$ mass difference. Equation (70) works far better than it should, as not only are the "heavy" quarks involved not all that heavy, but even the statement that the wave function at the origin squared is proportional to the reduced mass is only approximate. Such superb agreement must be an accident.

Now let us return to systems with two heavy quarks. There the wave functions are not determined by the linear part of the potential and Eq. (70) should not hold. (It doesn't!) But here we can be

braver yet and insert $v(r) = -4\pi\alpha_s/r$ into Eq. (65) and sandwich it between ground state vector and pseudoscalar meson wave functions to obtain[68]

$$M(^3S_1) - M(^1S_0) = \frac{32\pi\alpha_s}{9}\,\frac{|\Psi(0)|^2}{m^2}\,\left(1 + \mathcal{O}(\frac{\alpha_s}{\pi})\right), \qquad (71)$$

where even the next order QCD corrections have been calculated. If we take the measured splitting between the ψ and η_c and invert Eq. (71) to find α_s, the result[zz31] is 0.3 to 0.4. This is perhaps a little bit too big, not to be regarded as very significant at this time.

- The Spin-Orbit and Tensor Interactions

Spin-orbit terms give rise to the fine structure in the old atomic physics terminology. In the case of equal constituent masses they take the form

$$V_{S.O.} = \frac{\vec{S}\cdot\vec{L}}{2m^2}\,\left(-\frac{ds(r)}{rdr} + 3\frac{dv(r)}{rdr}\right), \qquad (72a)$$

and

$$V_{Tensor} = \frac{1}{12m^2}\left(6\vec{S}\cdot\hat{r}\vec{S}\cdot\hat{r} - 2\vec{S}\cdot\vec{S}\right)\,\left(\frac{dv(r)}{rdr} - \frac{d^2v(r)}{d^2r}\right). \qquad (72b)$$

If we take the spin-orbit and tensor interactions and calculate their contributions to the ^3P_J state masses, we get[69]

$$M(^3P_2) = \vec{M} + a - 2b/5 \qquad (73a)$$

$$M(^3P_1) = \vec{M} - a + 2b \qquad (73b)$$

$$M(^3P_0) = \vec{M} - 2a - 4b, \tag{73c}$$

where the matrix elements a and b are defined as

$$a = \frac{1}{2m^2}\left\langle -\frac{ds}{rdr} + 3\frac{dv}{rdr}\right\rangle, \tag{74a}$$

$$b = \frac{1}{12m^2}\left\langle \frac{dv}{rdr} - \frac{d^2v}{dr^2}\right\rangle. \tag{74b}$$

We can summarize the relative values of the matrix elements in terms of one number by forming the ratio

$$r = \frac{M(^3P_2) - M(^3P)_1}{M(^3P_1) - M(^3P_0)} = \frac{2a - \frac{12}{5}b}{a + 6b}. \tag{75}$$

If only the spin-orbit term contributes, $r = 2$, while if the Coulomb-like vector part of the potential $v(r)$ is present, $r = 0.8$. As one turns on the scalar term, $s(r)$, the matrix element a decreases, as does r.

If you look at the experimental numbers,[38] updated with recent data, particularly from CUSB,[70] one finds[38] for charmonium $r_{\chi_c} = 0.50 \pm 0.02$, and for bottomonium $r_{\chi_b} = 0.67 \pm 0.05$ and $r_{\chi_b'} = 0.70 \pm 0.20$, for the 1P and 2P states, respectively. All these values are smaller than would result from solely a Coulomb-like vector term, and point toward a non-negligible scalar term. Moreover, the detailed predictions from taking the vector term as $-\frac{4}{3}\alpha_s/r$ and the scalar term as kr give quite good agreement[71] with the data, particularly for bottomonium (recall that one expects some corrections, particularly for charmonium). The case is getting fairly good for a substantial part of the long range, confining part of the potential being scalar rather than vector.

For mesons composed of a heavy quark and a light antiquark or *vice versa* the physical situation is different, as we discussed previously in considering the spin-spin interaction. The light quark lives at larger distances, so that the Thomas term, $-ds(r)/rdr$, can "beat" the net vector term, $3dv(r)/rdr$, and the effect of the spin orbit interaction, $\langle V_{S.O.} \rangle$, can be reversed in sign. This would result in an inversion of spin multiplets[72] compared to atomic physics, charmonium, and bottomonium where the higher spin state lies higher: the ordering would now be $M(^3P_0) > M(^3P_1) > M(^3P_2)$. This idea might be testable in the ^3P charm meson states, labelled here D^{**}'s. A candidate state, the $D^{**}(2420)$, already has been found and must be $J = 1$ or 2, as it decays to $D^*\pi$. If this multiplet is inverted, the $J = 0$ state, which decays to $D\pi$, will lie at a higher mass than the $D^{**}(2420)$.

- Conclusion

In this brief and incomplete review of the spectroscopy of heavy quark systems, we have seen that we have a good qualitative picture of the nature of the spin-independent forces. That, plus some phenomenological potentials inspired by fundamental theory, carry us a long way. For the spin-dependent effects we even have a semi-quantitative understanding, as they are more sensitive to the short distance part of the potential and we have more insight and more tools to help us sort things out.

Eventually, we want a quantitative calculation of both the spin-independent potential $V(r)$ and the spin-dependent potentials $V_2(r)$, $V_3(r)$, and $V_4(r)$, from QCD. This will likely come in due time from improvements in computer power and in technique over the present lattice calculations.

In the meantime, to clarify the emerging picture, we need more data. We need to find or confirm the $^1P_1$ states of charmonium and bottomonium. We need to find the η_b. We need to find the other D^{**}'s. And maybe best of all, we need to see the spectrum of toponium.

6. RADIATIVE TRANSITIONS

As in our earlier discussion of charmonium spectroscopy, we assume that we are dealing with heavy quarks for which the non-relativistic, two-body bound state regime is a good approximation of reality. Radiative transitions between levels then occur preferentially through the emission of photons in the lowest multipole consistent with the spin and parity of the initial and final hadronic states.

The various radiative transitions for charmonium are shown in Figure 12 and those for bottomonium in Figure 13. Transitions of the form $^3P \rightarrow {}^3S + \gamma$ or $^3S \rightarrow {}^3P + \gamma$ are electric dipole in character, while $^3S \rightarrow {}^1S + \gamma$ transitions are magnetic dipole. The corresponding rates behave as

$$\Gamma_{E1} \propto e_Q^2 (2J_f + 1)\ k_\gamma^3 \mid < f | \overrightarrow{r} | i > |^2, \tag{76}$$

and

$$\Gamma_{M1} \propto e_Q^2 (2J_f + !)\ k_\gamma^3 \mid < f | \overrightarrow{\sigma} / 2M_Q | i > |^2, \tag{77}$$

respectively.

Table V summarizes[38] the situation for electric dipole transitions of the type $2^3S_1 \rightarrow \gamma\, 1^3P_J$, *i. e.*, $\psi' \rightarrow \gamma\, \chi_J$. One sees that the simple

TABLE V

RADIATIVE TRANSITIONS[38] FROM THE ψ' TO THE χ STATES

Transition	$\Gamma_{Experiment}$ (keV)	Γ_{NR} (keV)	Γ_{CC} (keV)	Γ_{REL} (keV)
$\psi' \rightarrow \gamma\chi_0$	20.1 ± 4	45	16	19
$\psi' \rightarrow \gamma\chi_1$	18.6 ± 4	40	23	31
$\psi' \rightarrow \gamma\chi_2$	16.8 ± 4	27	22	27

non-relativistic model predicts widths (Γ_{NR}) which are consistently about a factor of two bigger than the experimental widths.

There are two explanations for this discrepancy, both of which put theory and experiment in rough accord. One is in terms of coupled-channel effects (of the charmonium bound states to the open charm states above threshold), whose predictions[45] are indicated as Γ_{CC} in Table V. A second explanation comes from relativistic effects, an example[73] of which is given in Table V as Γ_{REL}. Both effects should be considerably less in the bottomonium system. This is indeed the case, as shown in Table VI, where the experimental widths for the transitions $\Upsilon' \rightarrow \gamma\ \chi_b$ are compared to the predictions, scaled to the correct photon energies, of one specific (relativistic) model,[74] although a number of theoretical models all give comparable results for these widths.[38]

Within the experimental errors, there is good agreement between theory and experiment - certainly there is no factor of two discrepancy here. A similar conclusion holds for the $\Upsilon'' \rightarrow \gamma\ \chi_b'$ transitions.[70]

TABLE VI

RADIATIVE TRANSITIONS[38] FROM THE Υ' TO THE χ_b STATES

Transition	$\Gamma_{Experiment}$ (keV)	$\Gamma_{Moxhay-Rosner}$ (keV)
$\Upsilon' \rightarrow \gamma\chi_{b,0}$	1.3 ± 0.4	1.0
$\Upsilon' \rightarrow \gamma\chi_{b,1}$	2.0 ± 0.5	2.1
$\Upsilon' \rightarrow \gamma\chi_{b,2}$	2.0 ± 0.5	2.2

This agreement for the more non-relativistic bottomonium case allows us to conclude that we are on the right track for charmonium. Another indication of this comes from the $1^3P_J \rightarrow \gamma\ 1^3S_1$, *i.e.*, $\chi \rightarrow \gamma\psi$ transitions in charmonium shown in Table VII.

TABLE VII

RADIATIVE TRANSITIONS[38] FROM THE χ STATES TO THE ψ

Transition	$\Gamma_{Experiment}$ (keV)	Γ_{NR} (keV)	Γ_{CC} (keV)	Γ_{REL} (keV)
$\chi_0 \rightarrow \gamma\psi$	95 ± 37	121	117	128
$\chi_1 \rightarrow \gamma\psi$	≤ 252	250	240	270
$\chi_2 \rightarrow \gamma\psi$	429^{+270}_{-169}	362	305	347

Although the experimental widths in Table VII are not pinned down with high accuracy (because the total widths of the χ states are not accurately known), all the calculations are in rough agreement with each other and with the data. The reason that the relativistic corrections have such a small effect here, but a large effect in the case of $\psi' \to \gamma\ \chi_J$, is shown in Figure 14. We see that the matrix element for $2S \to 1P$ electric dipole transitions involves a cancellation which is sensitive to the position of the node in the $2S$ wave function, something which is shifted by the relativistic corrections.[73] This does not occur for matrix elements for $2P \to 1S$ transitions, which are relatively insensitive to corrections.

The situation for magnetic dipole transitions between charmonium levels is shown in Table VIII. We recall that the $\psi \to \gamma\eta_c$ and $\psi' \to \gamma\eta_c'$ transitions involve a flip of the quark spin, but the same spatial wavefunction in the initial and final states in a non-relativistic picture. This makes the calculation rather unambiguous, aside from deciding what value to assign to the charm quark mass in the expression for the magnetic dipole matrix element. Within their respective errors, theory and experiment are in rough agreement.

The transition $\psi' \to \gamma\eta_c$ on the other hand is of the form $2^3S_1 \to 1^1S_0$, and involves a $2S-1S$ wavefunction overlap which is zero in the non-relativistic limit. Indeed, there is a factor of 175 from the k_γ^3 factor favoring this transition over $\psi \to \gamma\eta_c$; yet Table VIII shows they have roughly the same width. There must be an order of magnitude suppression in the matrix element. As such, the absolute prediction of the rate is very sensitive to relativistic and other effects; the theoretical prediction for this transition in Table VIII has intentionally been left blank, although it is possible to obtain agreement[45,73] with

TABLE VIII

MAGNETIC DIPOLE RADIATIVE TRANSITIONS FOR CHARMONIUM

Transition	$\Gamma_{Experiment}$ (keV)	Γ_{Theory} (keV)
$\psi \to \gamma\eta_c$	0.8 ± 0.24	~ 2
$\psi' \to \gamma\eta_c'$	$0.4 - 2.9$	~ 1
$\psi' \to \gamma\eta_c$	0.6 ± 0.13	

the experimentally measured decay rate. Nevertheless, the strong suppression of the matrix element observed experimentally should be taken as one more indication that the underlying picture of a bound, non-relativistic $\bar{c}c$ system is a good first approximation to the physics of charmonium.

7. HADRONIC TRANSITIONS

The most remarkable fact about hadronic transitions between onium states is that they have such small widths. After all, the ordinary hadrons (pions, etas) emitted in such decays have a low combined invariant mass; these are strong interaction processes in a regime where the running coupling is large. The reason[56] for the small widths emerges when we consider these transitions as occurring through the emission of gluons which later manifest themselves as ordinary hadrons. Each gluon "sees" the color carried by the quark and antiquark in a heavy $\bar{Q}Q$ system. However, the system as a

whole is a color singlet. As its size shrinks to zero, a gluon will "see" no net color; the amplitude for the transition will also go to zero.

Not only does this give us a simple understanding of the small rates for such processes, but it suggests an expansion in the size of the system, i. e., a multipole expansion,[75–79] in which the leading term (proportional to the total color charge) is zero. The first non-zero term involves the emission of two gluons and is of dipole - dipole character, with the form[78]

$$M_{E1-E1} \propto g_s^2 < \Phi_f | \vec{r} \cdot \vec{E}^{\alpha} \frac{1}{E_i - H_8 - iD} \vec{r} \cdot \vec{E}^{\alpha} | \Phi_i >, \quad (78)$$

where the index α runs over the eight gluons, the Hamiltonian H_8 describes the intermediate state where the $\bar{Q}Q$ system is in a color octet state, and D is the time component of the covariant gauge theory derivative. The explicit occurence of two powers of r in Eq. (78) shows how the small size of heavy onia enters the amplitude and makes it small. For $M1 - M1$ transitions, the transition amplitudes are small because $1/M_Q^2$ is small.

It is very difficult to calculate absolute rates in this situation, as we know neither the spectrum of H_8 nor the amplitude for the two gluons to turn into specific final hadrons. We can still maintain predictive power, but avoid these issues, by taking ratios of amplitudes. A prime example is provided by the processes $\psi' \to \psi\pi\pi$ and $\Upsilon' \to \Upsilon\pi\pi$. We have the additional piece of luck that the phase space available for the $\pi\pi$ system is almost the same in these two processes. Thus everything in the expressions for the respective amplitudes is nearly the same except the expectation value of the two powers of r that occur in the dipole - dipole matrix element. Therefore,

one expects[75,79]

$$\frac{\Gamma(\psi' \to \psi\pi\pi)}{\Gamma(\Upsilon' \to \Upsilon\pi\pi)} \sim \left[\frac{< r^2 >_{\psi'}}{< r^2 >_{\Upsilon'}}\right]^2, \tag{79}$$

with the right-hand-side found[79] to be ~ 16 from calculations using explicit bound state wave functions for the ψ' and Υ'. The present data for the left-hand-side are in good accord with this number.[38]

This agreement is an important verification of the basic idea that these hadronic transitions are small because of the small size of the onium system; the $\Upsilon' \to \Upsilon$ transition is smaller because the bottomonium system is smaller.

Bottomonium hadronic transitions are shown in Figure 15 (the charmonium transitions were contained in Figure 12). Table IX contains an abreviated selection of predictions for hadronic transitions in the bottomonium system, many of them obtained[79] by using the corresponding charmonium transition rate together with the multipole expansion to relate their amplitudes.

The $\pi\pi$ transitions among the Υ family have been partly dealt with above, and are in general accord with experiment. The transition $\Upsilon' \to \Upsilon\eta$ is particularly interesting because it is of $M1 - M1$ type, scales like $1/M_Q^2$, and should be detectable at the predicted rate. There are 9 possible transitions between the $2P$ and $1P$ states, but only 3 independent amplitudes in the multipole expansion. Thus there are 6 relations among the rates, which, however, are disappointingly small for experimental testing. The last transition in the Table is the best way to find the $^1P_1$ state, and may have already been observed (see Section 4).

TABLE IX

PREDICTIONS FOR HADRONIC TRANSITIONS
BETWEEN BOTTOMONIUM LEVELS

	Branching Ratio (%)	
Hadronic Transition	Theory[78,79]	Experiment[38]
$\Upsilon' \to \Upsilon\ \pi\pi$	$25-30$	27.4 ± 1.5
$\Upsilon' \to \Upsilon\ \eta$	0.04	< 0.2
$\Upsilon'' \to \Upsilon\ \pi^+\pi^-$	$2-5$	4.5 ± 0.8
$\Upsilon'' \to \Upsilon'\ \pi^+\pi^-$	$2-3$	3.1 ± 2.0
$2^3P_J \to 1^3P_J\ \pi\pi$	$0.1-0.3$	
$2^3P_J \to 1^3P_{J'}\ \pi\pi$	~ 0.01	
$1^3D_1 \to \Upsilon\ \pi\pi$	20 keV/Γ	
$\Upsilon'' \to {}^1P_1\ \pi\pi$	< 1	

There are also a number of hadronic transitions in the charmonium system that have small branching ratios, but may well be observable. Among them are: $\psi'' \to \eta_c\ \omega$ involving three gluons (and very small?); $\psi'' \to \psi\pi\pi$, which must occur at least through the 2^3S_1 component of the ψ''; $1^3D_2 \to \psi\pi\pi$ and $1^1D_2 \to \eta_c\pi\pi$, which involve narrow charmonium states above $\bar{D}D$ (into which they can not decay) but not $\bar{D}D^*$ threshold; and $\eta_c' \to \eta_c\ \pi\pi$, which should have approximately the same width ($\sim$ 100 keV) as $\psi' \to \psi\pi\pi$, but a much smaller ($\sim$ 2%) branching ratio because of the much larger width of the η_c'.

8. CHARM PRODUCTION ABOVE OPEN CHARM THRESHOLD

Once we cross open charm threhold at 3.73 GeV, a wealth of interesting new phenomena occur in e^+e^- annihilation. We still have the continuation of the charmonium levels, the 3^3S_1, 4^3S_1,... and

1^3D_1, 2^3D_1,... states with $J^P = 1^-$. In addition, there may be "mixed" states[80] of the form $\bar{c}cg$ with these quantum numbers. These have been actively looked for in the bottom[81] system without success, but they may well be lurking in the region above 4 GeV in the center-of-mass for charm.

In addition to this there may be "charm molecules" with the quark content of $\bar{c}c\bar{q}q$, or more accurately, $(\bar{c}q)(\bar{q}c)$, as these are quasi-bound states of $\bar{D}D$, $\bar{D}D^*$, *etc.*, just above their thresholds.[82] Even without resonant states there may be enhancements in various channels just above their respective thresholds.

The continuum itself rapidly becomes fairly complicated. Even restricting ourselves to production of two-body or quasi-two-body final states, we have:

- $\bar{D}D$, $\bar{D}D^* + \bar{D}^*D$, $\bar{D}^*D^*$, $\bar{D}D^{**}$,... where D^{**} indicates an $L = 1$ charm state which decays to πD and/or πD^*;
- $\bar{D}_sD_s$, $\bar{D}_sD_s^* + \bar{D}_s^*D_s$, $\bar{D}_s^*D_s^*$, $\bar{D}_sD_s^{**}$,... where the D_s^{**} indicates and $L = 1$ charm-strange state that decays to $\pi\pi D_s$ (a suppressed strong interaction decay) or, if allowed, to $D\ K$ and/or $D^*\ K$;
- $\bar{\Lambda}_c\Lambda_c$, $\bar{\Sigma}_c\Sigma_c$, $\bar{\Sigma}_c\Sigma_c^*$,... including the production of a lowest $L = 1$ charmed baryon with a mass of $\sim$ 2500 MeV, which may be forbidden to decay strongly,[83] and therefore has the dominant decay $\Lambda_c' \to \gamma\ \Lambda_c$;
- $\bar{\Xi}_c\Xi_c$, $\bar{\Xi}_c\Xi_c^*$,...

The interplay of the continuum and the resonances is a whole subject in itself.[84] A representative decomposition from one calculation[45] of the part of the charm production cross section that involves D

mesons is shown in Figure 16. Note in particular the valleys in particular channels produced by overlaps of wave functions with radial nodes. For comparison, one set of experimental measurements[85] of the total e^+e^- annihilation cross section into hadrons is shown in Figure 17.

With all this in mind, let us start from open charm threshold and make our way upward in energy, highlighting some of the open questions:

- The $\psi''(3.77)$ is a "D factory" which dominantly decays to $\bar{D}D$ and is dominantly a $^3D_1$ state with a small admixture of $^3S_1$. How big are decays like $\psi'' \to \psi\pi\pi$ and $\psi'' \to \gamma\ \chi$ of the ψ'' into other charmonium states?
- As noted before, the $^3D_2$ and $^1D_2$ states should be narrow as they likely lie near the ψ'', are forbidden to decay into $\bar{D}D$, and are probably below threshold for decay into $\bar{D}D^*$. They are not directly produced in e^+e^-, but could be found in $\bar{p}p$ experiments and have interesting decays into other charmonium states.
- There is a local maximum in the cross section around ~ 3.96 GeV, not far above $\bar{D}D^*$ threshold (see Figure 17). Is this indeed some sort of enhancement associated with $\bar{D}D^*$, or is it associated with $\bar{D}_sD_s$ threshold, which we now know is also very nearby?
- The $\psi(4.03)$ is a clear peak (see Figure 17) with a major decay into $\bar{D}^*D^*$ even though this channel has just opened, but its character as a $3S$ charmonium level, charm molecule, or something else remains to be settled.

- The $\psi(4.16)$ is another peak. It is at too low an energy to be the $4S$ state. Does it have anything to do with $\bar{D}_s D_s^*$ threshold which is just below it?
- There is a long valley in the cross section with a minimum at $\sim$ 4.3 GeV. Is there no enhancement above $\bar{D}_s^* D_s^*$ threshold, which lies in this region?
- The $\psi(4.415)$ would seem to be a good candidate for the $4S$ state of charmonium. Does it decay to $\bar{D}D^{**}$?
- Charmed baryon threshold is at $\sim$ 4.57 GeV, and experiments just above this energy have the capability of making an absolute branching ratio measurement for the Λ_c if enough decays can be "tagged". At energies above $\sim$ 5 GeV, the charmed-strange baryons (Ξ_c) should be produced, as well as Σ_c, Σ_c^*, and other excited charmed baryons. The production and weak decays of charmed baryons is a subject that has barely been touched.

REFERENCES

1. M. Witherell, these Proceedings.
2. D. G. Hitlin, these Proceedings.
3. I. Bigi, these Proceedings.
4. W. Toki, these Proceedings.
5. M. S. Chanowitz, these Proceedings.
6. S. Weinberg, Phys. Rev. Lett. 19, 1264 (1967); A. Salam, *Proceedings of the Eighth Nobel Symposium*, edited by N. Svartholm (Almqvist and Wiksell, Stockholm, 1968), p. 367.
7. See the excellent recent review by P. Langacker, in *Proceedings of the 1985 Int. Symp. on Lepton and Photon Interactions at High Energies*, edited by M. Konuma and K. Takahashi (Kyoto University, Kyoto, 1986), p. 186. The latest review is found in U. Almaldi *et al.*, University of Pennsylvania preprint UPR-0331T, 1987 (unpublished).
8. M. Kobayashi and T. Maskawa, Prog. Theor. Phys. 49, 652 (1973).
9. Particle Data Group, Phys. Lett. 170B, 74 (1986).
10. W. J. Marciano and A. Sirlin, Phys. Rev. Lett. 56, 22 (1986).
11. H. Leutwyler and M. Roos, Z. Phys. C25, 91 (1984).
12. H. Abramowicz *et al.*, Z. Phys. C15, 19 (1982).
13. The c and b decay data at that time were reviewed by E. Thorndike, in *Proceedings of the 1985 International Symposium on Lepton and Photon Interactions at High Energies*, edited by M. Konuma and K. Takahashi (Kyoto University, Kyoto, 1986), p. 406. For a review of the experimental situation as of the summer of 1986 see M. G. D. Gilchriese, rapporteur talk in *Proceedings of the XXIII International Conference on High Energy Physics*, edited by S. C. Loken (World Scientific, Singapore, 1987), p. 140.
14. K. Kleinknecht and B. Renk, Mainz preprint MZ-ETAP/86-4, 1986 (unpublished).
15. A. Sirlin and R. Zucchini, Phys. Rev. Lett. 57, 1994 (1986).

16. E. G. Drukarev and M. I. Strikman, Leningrad Institute of Nuclear Physics preprint, No. 1221, 1986 (unpublished).

17. I thank Bill Marciano for a clarifying discussion of the comparison of the two new results.

18. Some recent reviews from various viewpoints are found in A. J. Buras, Max Planck Institute preprint MPI-PAE/PTH 40/86, 1986 (unpublished); R. Ruckl, in *Proceedings of the XXIII International Conference on High Energy Physics*, edited by S. C. Loken (World Scientific, Singapore, 1987), p. 797; I. Bigi, Phys. Lett. 169B, 101 (1986) and Ref. 3.

19. M. K. Gaillard and B. W. Lee, Phys. Rev. Lett. 33, 108 (1974); G. Altarelli and L. Maiani, Phys. Lett. 52B, 351 (1974).

20. The discussion which follows parallels that of F. J. Gilman and M. B. Wise, Phys. Rev. D20, 2392 (1979).

21. M. A. Shifman *et al.*, Zh. Eksp. Teor. Fiz. Pis'ma Red. 22, 123 (1975) [JETP Lett. 22, 55 (1975)]; M. A. Shifman *et al.*, Nucl. Phys. B120, 316 (1977).

22. See, for example, F. J. Gilman, in the *Second Aspen Winter Particle Physics Conference*, Annals of the New York Academy of Sciences, Vol. 490, edited by L. Durand (The New York Academy of Sciences, New York, 1987), p. 1; and A. J. Buras, W. A. Bardeen, and J. M. Gerard, Phys. Lett. 180B, 133 (1980) and Max Planck Institute preprints MPI-PAE/Pth-45/86 and MPI-PAE/Pth-55/86, 1986 (unpublished).

23. B. Guberina, R. D. Peccei, and R. Ruckl, Phys. Lett. 90B, 169 (1980).

24. For a recent calculation of "penguin" effects in exclusive B decays see M. B. Gavela *et al.*, Phys. Lett. 154B, 425 (1985).

25. M. L. Perl, Ann. Rev. Nucl. Part. Sci. 30, 299 (1980).

26. In the following we take the properties of the tau, unless otherwise specified, from the review of J. G. Smith, invited talk at the 1987 Spring Meeting of the American Physical Society, Bulletin of the American Physical Society, Series II, 32, No. 4, p. 1010, 1987 (unpublished). The situation as of the summer of 1986 is found in M. G. D. Gilchriese, Ref. 13.

27. H. Albrecht *et al.*, Phys. Lett. 185B, 228 (1987).

28. Y. S. Tsai, Phys. Rev. D4, 2821 (1971); H. B. Thacker and J. J. Sakurai, Phys. Lett. 36B, 103 (1971).

29. F. J. Gilman and D. H. Miller, Phys. Rev. D17, 1846 (1978) and unpublished calculations with the present value of M_τ.

30. F. J. Gilman and S. H. Rhie, Phys. Rev. D31, 1066 (1985) and references to other previous work therein.

31. H. Albrecht *et al.*, Phys. Lett. 185B, 223 (1987).

32. F. J. Gilman, SLAC preprint SLAC-PUB-4365, 1987 and Phys. Rev., in press.

33. P. R. Burchat *et al.*, Phys. Rev. D35, 27 (1987); H. Aihara *et al.*, Phys. Rev. Lett. 57, 1836 (1986); K. K. Gan *et al.*, SLAC preprint SLAC-PUB-4110, 1987 (unpublished).

34. S. Keh *et al.* and S. Abachi *et al.*, contributions to the Berkeley Conference quoted in M. G. D. Gilchriese, Ref. 13.

35. M. Derrick *et al.*, Phys. Lett. 189B, 260 (1987).

36. E. L. Berger and H. J. Lipkin, Phys. Lett. 189B, 226 (1987); Y. Meurice and C. K. Zachos, Mod. Phys. Lett. A 2, 247 (1987).

37. The ARGUS collaboration has set an upper limit of 1.3 % at 95% CL on the branching fraction for $\tau^- \to \nu_\tau \pi^- \eta$ (talk at the XXIInd Rencontre de Moriond, Les Arcs, France, March 8 - 16, 1987). The TPC collaboration set an upper limit on the branching fraction of the $SU(3)$ related decay, $\tau^- \to \nu_\tau K^- K^0$, of 0.26% (H. Aihara *et al.*, LBL preprint LBL-23176, 1987 (unpublished)). Also, the Mark III collaboration, D. Coffman *et al.*, SLAC preprint SLAC-PUB-4314, 1987 (unpublished), set a limit of 2.5%.

38. R. Schindler, in *Proceedings of the 14th SLAC Summer Institute on Particle Physics*, SLAC Report No. 312, edited by Eileen Brennan (SLAC, Stanford, 1987), p. 239 reviews much of the data relevant to the discussion here. See also W. Toki, Ref. 4.

39. Recent reviews are to be found in A. Martin, Comm. Nucl. Part. Phys. 16, 249 (1986) and W. Kwong, J. L. Rosner, and C. Quigg, University of Chicago preprint EFI 86-60, 1986 (to be published in Ann. Rev. Nucl. Part. Sci 37, 1987.

40. The basics and earlier accomplishments of lattice QCD calculations are set out in M. Creutz, *Quarks, Gluons, and Lattices* (Cambridge University Press, Cambridge, 1983).

41. S. Capstick, N. Isgur, and J. Paton, Phys. Lett. 175B, 457 (1986).

42. Relativistic corrections have been considered, for example, by P. Moxhay and J. L. Rosner, Phys. Rev. D28, 1132 (1983) and by R. McClary and N. Byers, Phys. Rev. D28, 1692 (1983). The effects of light quark pairs are studied by N. Byers and V. Zambetakis, invited talk at the Second Conference on Interactions Between Particle and Nuclear Physics, Lake Louise, Canada, May 23-32, 1986 and UCLA preprint UCLA/86/TEP/24, 1986 (unpublished).

43. The sum rule approach is reviewed by L. J. Reinders, H. Rubinstein, and S. Yazaki, Phys. Rep. 127, 1 (1985); and by M. A. Shifman, Ann. Rev. Nucl. Part. Sci 33, 199 (1984).

44. J. D. Jackson, *Proceedings of the Summer Institute on Particle Physics*, SLAC Report No. 198, edited by M. C. Zipf (SLAC, Stanford, 1976), p. 147.

45. E. Eichten *et al.*, Phys. Rev. D17, 3090 (1978) and D21, 203 (1980).

46. J. L. Richardson, Phys. Lett 82B, 272 (1979).

47. W. Buchmuller, G. Grunberg, and S. H. H. Tye, Phys. Rev. Lett. 45, 103 (1980); W. Buchmuller and S. H. H. Tye, Phys. Rev. D24, 132 (1981).

48. A. Martin, Phys. Lett. 93B, 338 (1980).

49. H. B. Thacker, C. Quigg and J. L. Rosner, Phys. Rev. D18 274 (1978) and D21, 234 (1980); C. Quigg and J. L. Rosner, Phys. Rev. D23, 2625 (1981).

50. B. Baumgartner, H. Grosse, and A. Martin, Phys. Lett. 146B, 363 (1984).

51. B. Baumgartner, H. Grosse, and A. Martin, Nucl. Phys. B254, 528 (1985).

52. P. J. Franzini and F. J. Gilman, Phys. Rev. D32, 237 (1985).

53. G. G. Athanasiu, P. J. Franzini, and F. J. Gilman, Phys. Rev. D32, 3010 (1985).

54. E. Eichten and F. Feinberg, Phys. Rev. D23, 2724 (1981).

55. E. Eichten, *Proceedings of the 11th SLAC Summer Institute on Particle Physics*, SLAC Report No. 267, edited by P. M. McDonough (SLAC, Stanford, 1983), p. 497.

56. M. Peskin, *Proceedings of the 11th SLAC Summer Institute on Particle Physics*, SLAC Report No. 267, edited by P. M. McDonough (SLAC, Stanford, 1983), p. 151.

57. D. Gromes, Z. Phys. C26, 401 (1984).

58. P. de Forcrand and J. D. Stack, Phys. Rev. Lett. 55, 1254 (1985); C. Michael, Phys. Rev. Lett. 56, 1219 (1985).

59. M. Campostrini, K. Moriarty, and C. Rebbi, Phys. Rev. Lett. 57, 44 (1986).

60. W. Buchmuller, Phys. Lett. 112B, 479 (1982). See also J. L. Rosner, J. de Phys. 46, C2, Supp. 2 (1985); R. D. Pisarski and J. D. Stack, Fermilab preprint FERMILAB-PUB -86/122-T, 1986 (unpublished), and M. G. Olsson and C. J. Suchyta, University of Wisconsin preprint MAD/PH/312, 1986 (unpublished).

61. C. Baglin *et al.*, Phys. Lett. 171B, 135 (1986).

62. T. Bowcock *et al.*, Phys. Rev. Lett. 58, 307 (1987).

63. C. Quigg and J. L. Rosner, Comm. Nucl. Part. Phys. 8, 11 (1978).

64. M. Frank and P. J. O'Donnell, Phys. Lett. 157B, 174 (1985).

65. H. J. Schnitzer, Phys. Lett. 134B, 253 (1984) and Brandeis preprint, 1985 (unpublished).

66. Particle Data Group, Phys. Lett. 170B, 1 (1986).

67. W. Toki, in *Proceedings of the 14th SLAC Summer Institute on Particle Physics*, SLAC Report No. 312, edited by Eileen Brennan (SLAC, Stanford, 1987), p. 495.

68. W. Buchmuller, Y. J. Ng, and S. H. H. Tye, Phys. Rev. D24, 3003 (1981); A. Martin and J. M. Richard, Phys. Lett. 115B, 323 (1982).

69. J. L. Rosner, *Proceedings of the 1985 Symposium on Lepton and Photon Interactions at High Energies*, edited by M. Konuma and K. Takahashi (Kyoto University, Kyoto, 1986), p. 448.

70. P. M. Tuts, in *Proceedings of the 14th SLAC Summer Institute on Particle Physics*, SLAC Report No. 312, edited by Eileen Brennan (SLAC, Stanford, 1987), p. 507.

71. See Table X of Ref. 1 and references to the original calculations there.

72. H. J. Schnitzer, Phys. Lett. 76B, 461 (1978). See also, J. L. Rosner, Comm. Nucl. Part. Phys. 16, 109 (1986).

73. R. McClary and N. Byers, Ref. 42.

74. P. Moxhay and J. L. Rosner, Ref. 42.

75. K. Gottfried, Phys. Rev. Lett. 40, 598 (1978).

76. G. Bhanot, W. Fischler, and S. Rudaz, Nucl. Phys. B155, 208 (1979).

77. M. E. Peskin, Nucl. Phys. B156, 365 (1979); G. Bhanot and M. E. Peskin, Nucl. Phys. B156, 391 (1979).

78. T.-M. Yan, Phys. Rev. D22, 1652 (1980).

79. Y.-P. Kuang and T.-M. Yan, Phys. Rev. D24, 2874 (1981).

80. R. C. Giles and S.-H. H. Tye, Phys. Rev. Lett. 37, 1175 (1976); Phys. Rev. D16, 1079 (1977); Phys. Lett. 73B, 30 (1978).

81. W. Buchmuller and S.-H. H. Tye, Phys. Rev. Lett. 44, 850 (1980).

82. A. De Rujula, H. Georgi, and S. L. Glashow, Phys. Rev. Lett. 38, 317 (1977).

83. L. A. Copley, N. Isgur, and G. Karl, Phys. Rev. D20, 768 (1979).

84. E. Eichten *et al.*, Phys. Rev. Lett. 36, 500 (1976) and Ref. 45.

85. J. Siegrist, SLAC Report No. 225, 1979.

FIGURE CAPTIONS

1. The spectrum of charmonium.
2. The spectrum of bottomonium.
3. Set of lowest order "penguin" graphs contributing to strange quark decay (upper left), Cabibbo suppressed charm quark decay (upper right), and Cabibbo suppressed bottom quark decay (lower left). Also shown is a spectator graph which also contributes to Cabibbo suppressed bottom quark decays (lower right).
4. Comparison of the shape of the Cornell[45] (dotted curve), Richardson[46,47] (solid curve), and Martin[48] (dash-dot curve) potentials. The inset shows the same comparison with the potentials displaced slightly on the vertical scale and a logarithmic horizontal scale, along with the mean radii of some charmonium and bottomonium states.
5. The spectrum of energy levels in the case of the Coulomb potential (a), the three dimensional harmonic oscillator (b), and a hybrid of the two (c).
6. The spectrum of nS states of toponium obtained[52] from the Richardson potential with m_t in the range of 40 to 50 GeV.
7. The value of the wave function at the origin for toponium nS states obtained[52] with the Richardson potential and m_t in the range of 40 to 50 GeV.
8. Results of a lattice Monte Carlo calculation[59] of the spin-dependent potential $-dV_1/dr$ as a function of radial distance in units of the lattice spacing, a.
9. Results of a lattice Monte Carlo calculation[59] of the spin-dependent potential dV_2/dr as a function of radial distance in units of the lattice spacing, a. The solid points are before, and the open points after a correction for lattice artifacts described in Ref. 59.
10. Results of a lattice Monte Carlo calculation[59] of the spin-dependent potential V_3 as a function of radial distance in units of the lattice spacing, a. The solid points are before, and the

open points after a correction for lattice artifacts described in Ref. 59.

11. Results of a lattice Monte Carlo calculation[59] of the spin-dependent potential $-V_4$ as a function of radial distance in units of the lattice spacing, a. The solid points are before, and the open points after a correction for lattice artifacts described in Ref. 59.
12. Radiative and hadronic transitions between charmonium levels.
13. Radiative transitions for bottomonium.
14. The $1S$, $2S$, and $1P$ wave functions showing the relative position of their nodes.
15. Hadronic transitions between bottomonium levels.
16. Decomposition of the charm cross section involving D mesons into its component channels according to Ref. 45.
17. The total cross section for e^+e^- annihilation into hadrons in units of the point cross section from Ref. 85. The arrows point to the positions of the $3S$ and $4S$ charmonium states in two theoretical calculations.

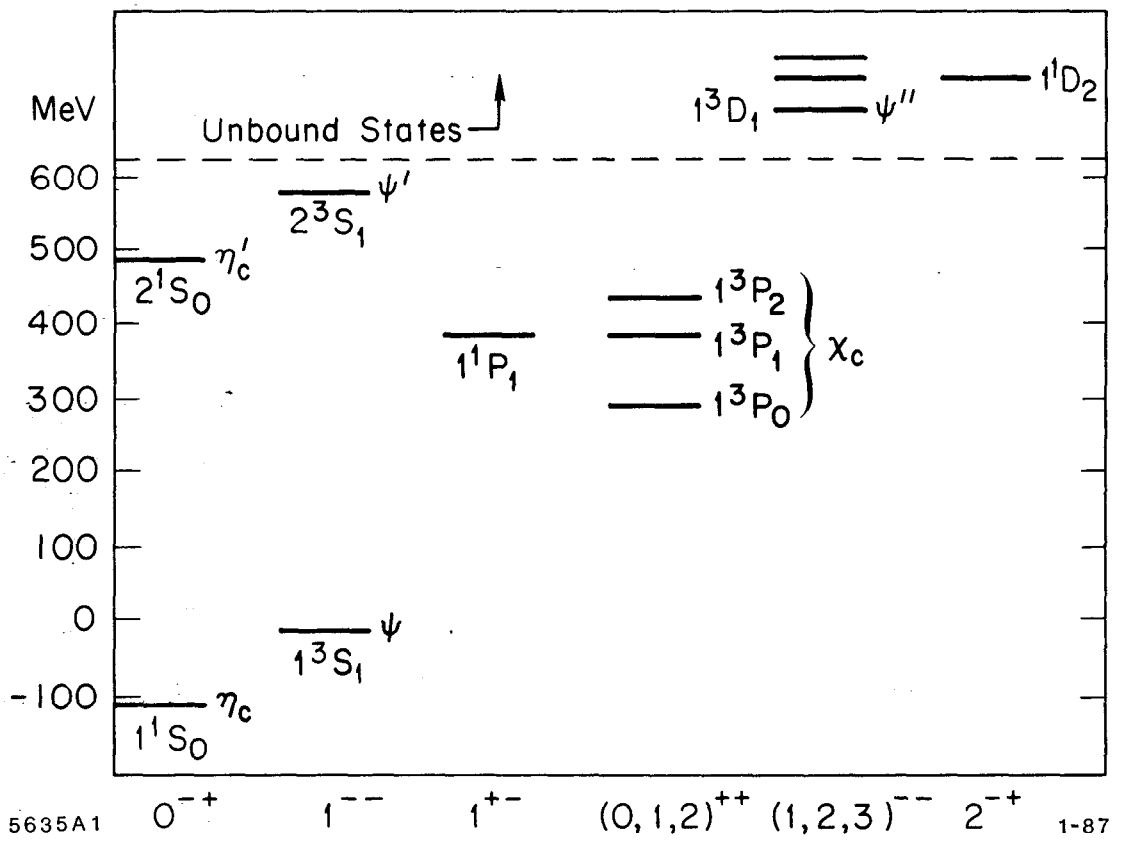
MeV
Unbound States
600
500
400
300
200
100
0
-100
2^3S_1 ψ'
2^1S_0 η_c'
1^1P_1
1^3P_2
1^3P_1
1^3P_0
χ_c
1^3S_1 ψ
1^1S_0 η_c
1^3D_1
ψ''
1^1D_2
0^{-+}
1^{--}
1^{+-}
$(0,1,2)^{++}$
$(1,2,3)^{--}$
2^{-+}
5635A1
1-87

Fig. 1

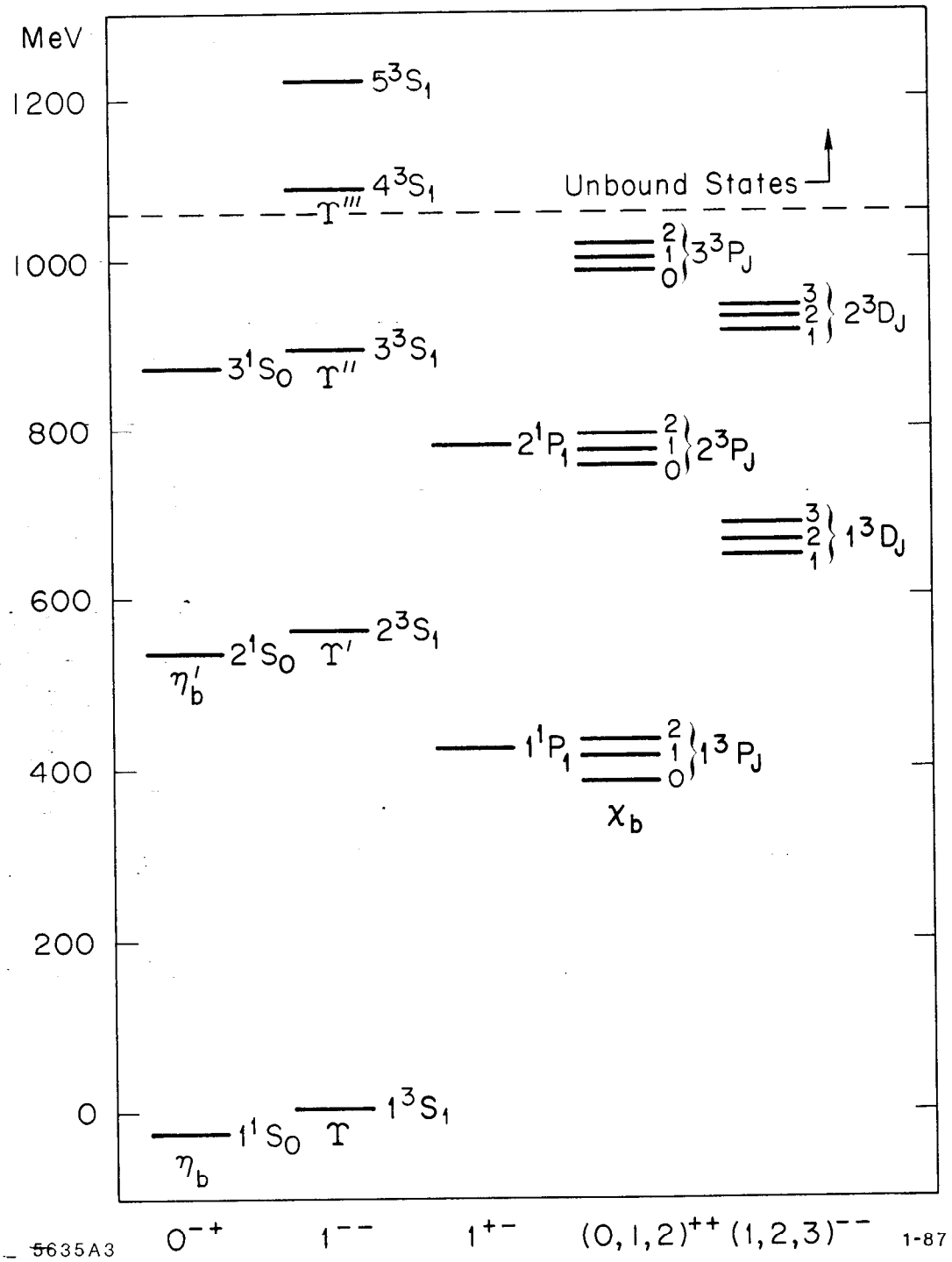
MeV
1200
1000
800
600
400
200
0
5^3S_1
4^3S_1
Υ'''
Unbound States
3^3P_J
2^3D_J
3^1S_0
Υ''
3^3S_1
2^1P_1
2^3P_J
1^3D_J
2^1S_0
η_b'
Υ'
2^3S_1
1^1P_1
1^3P_J
χ_b
1^1S_0
η_b
Υ
1^3S_1
0^{-+}
1^{--}
1^{+-}
$(0,1,2)^{++}$ $(1,2,3)^{--}$
5635A3
1-87

Fig. 2

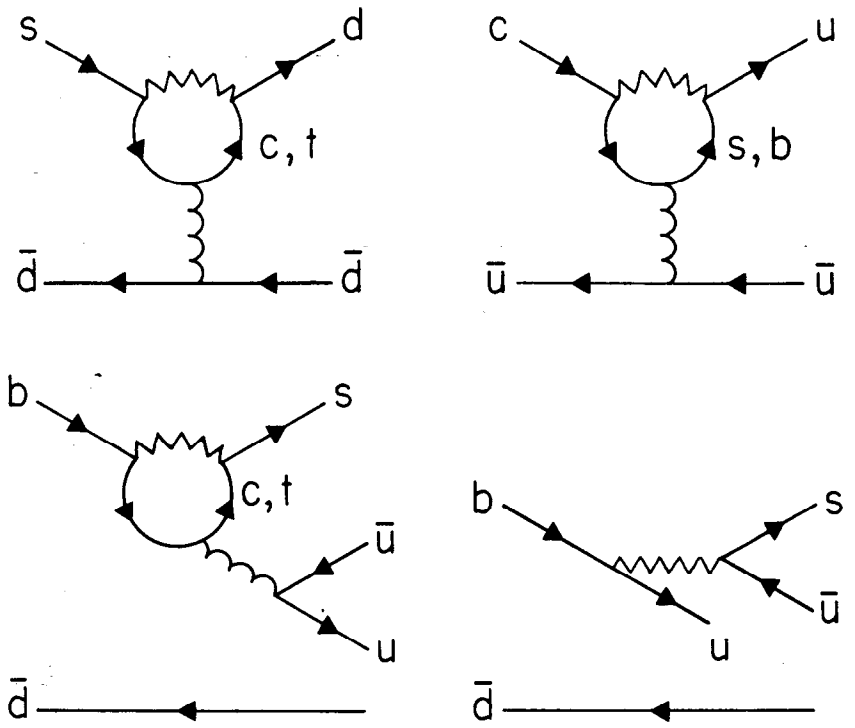

Fig. 3

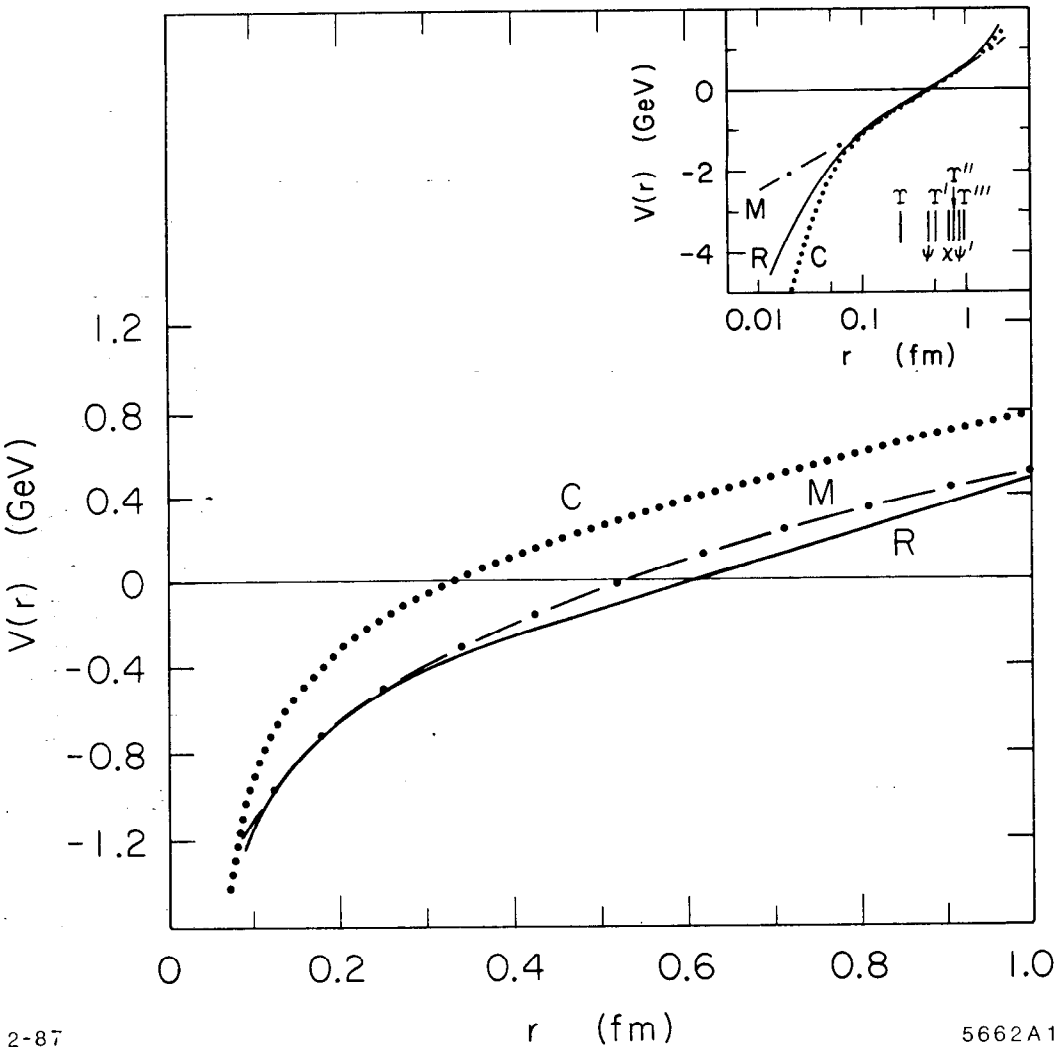
V(r) (GeV)
1.2
0.8
0.4
0
-0.4
-0.8
-1.2
C
M
R
0
0.2
0.4
0.6
0.8
1.0
r (fm)
2-87
5662A1
V(r) (GeV)
0
-2
-4
M
R
C
0.01
0.1
1
r (fm)
ϒ
ϒ′
ϒ″
ϒ‴
ψ
xψ′

Fig. 4

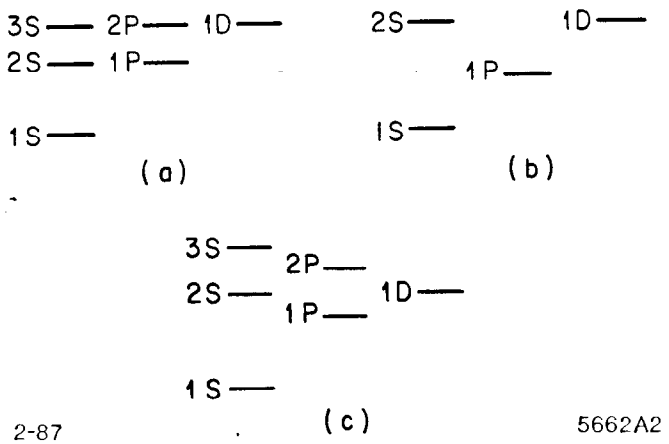

Fig. 5

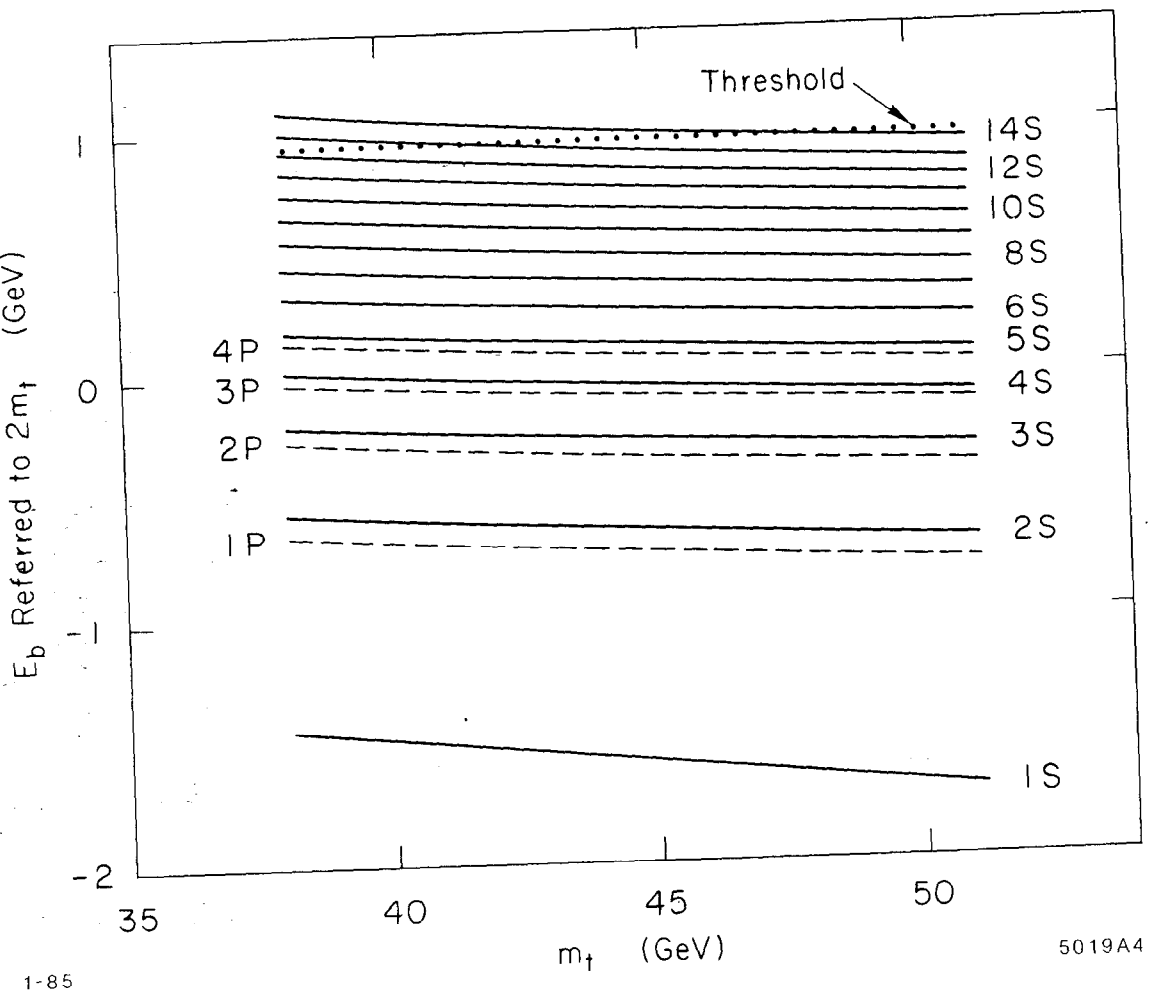
Threshold
14S
12S
10S
8S
6S
5S
4S
3S
2S
1S
4P
3P
2P
1P
1
0
-1
-2
35
40
45
50
E_b Referred to $2m_t$ (GeV)
m_t (GeV)
1-85
5019A4

Fig. 6

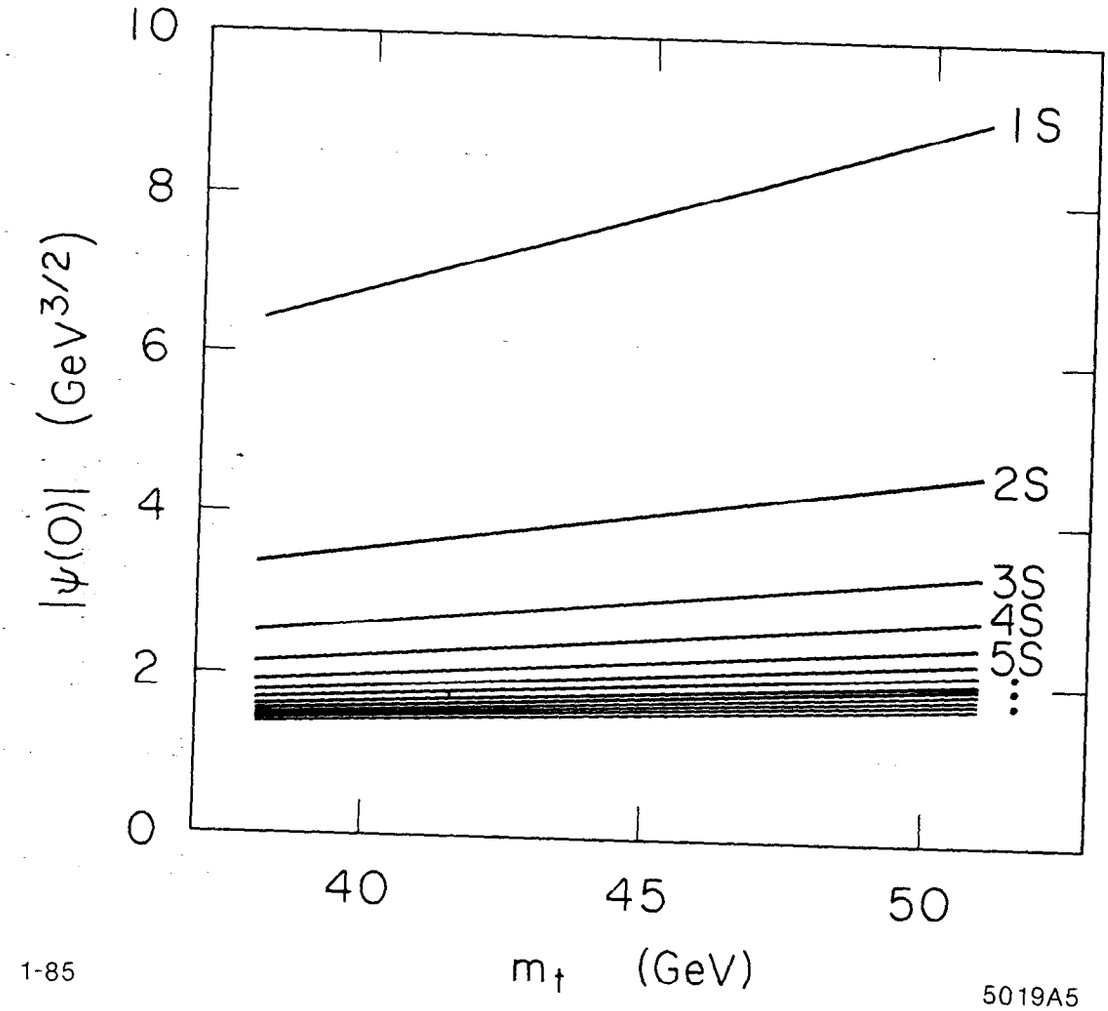

Fig. 7

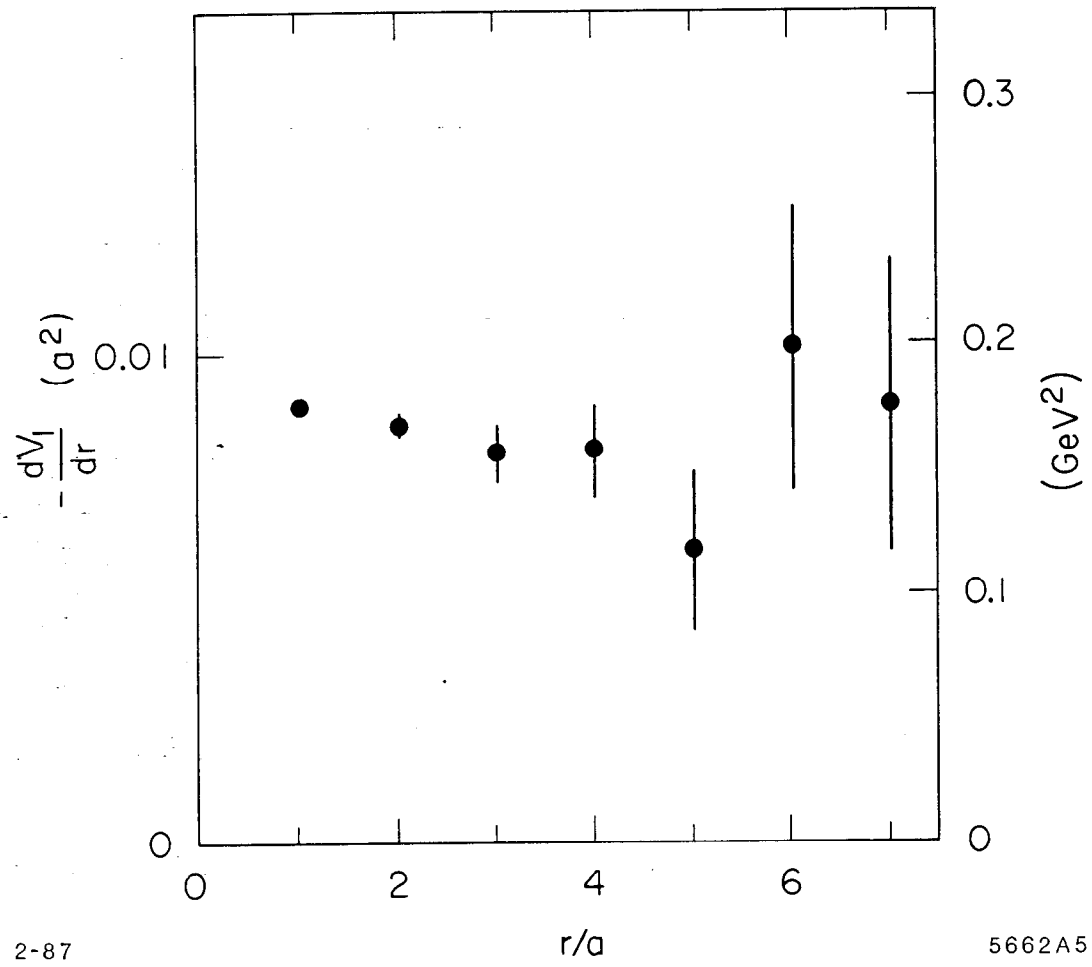

Fig. 8

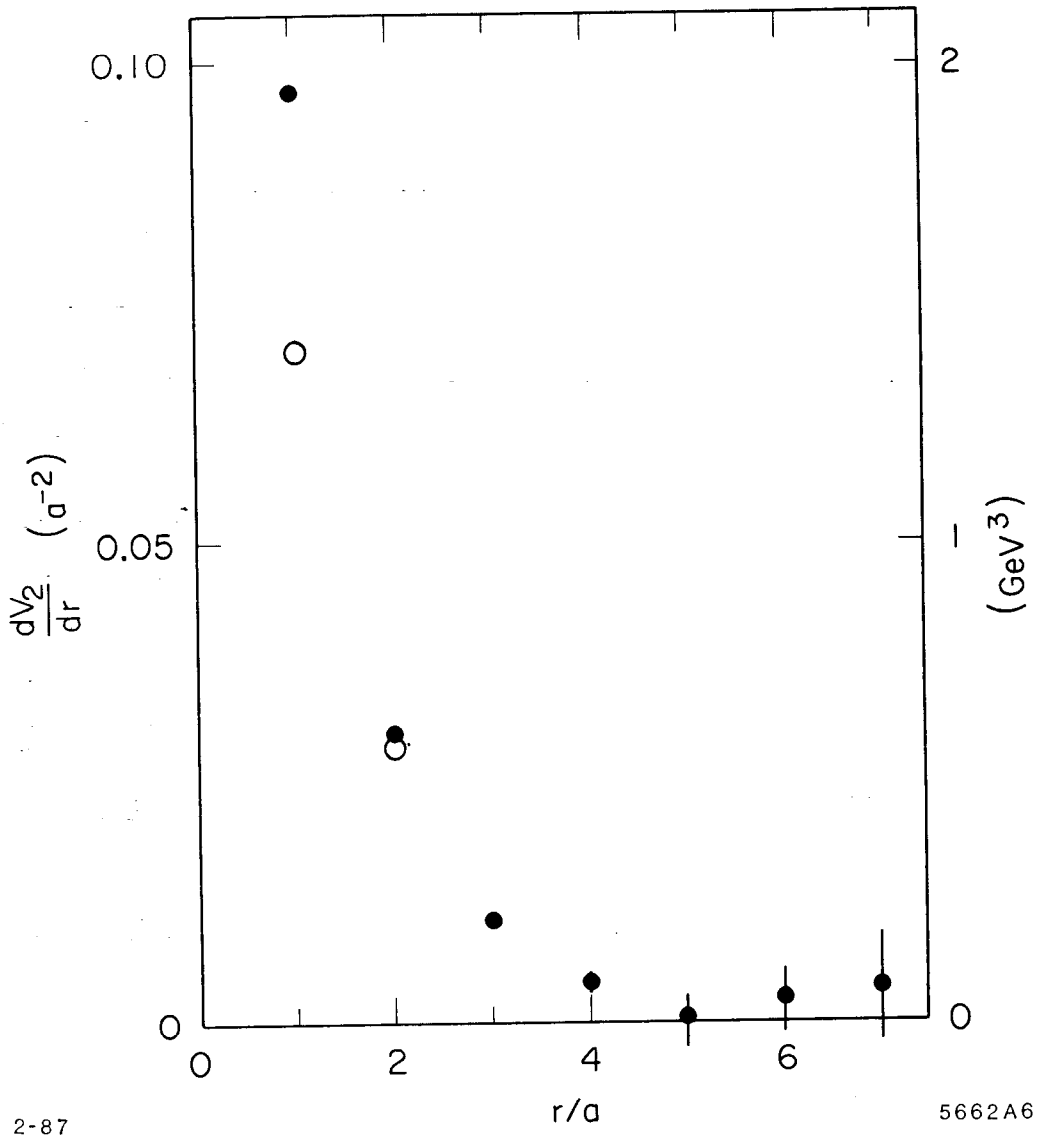

Fig. 9

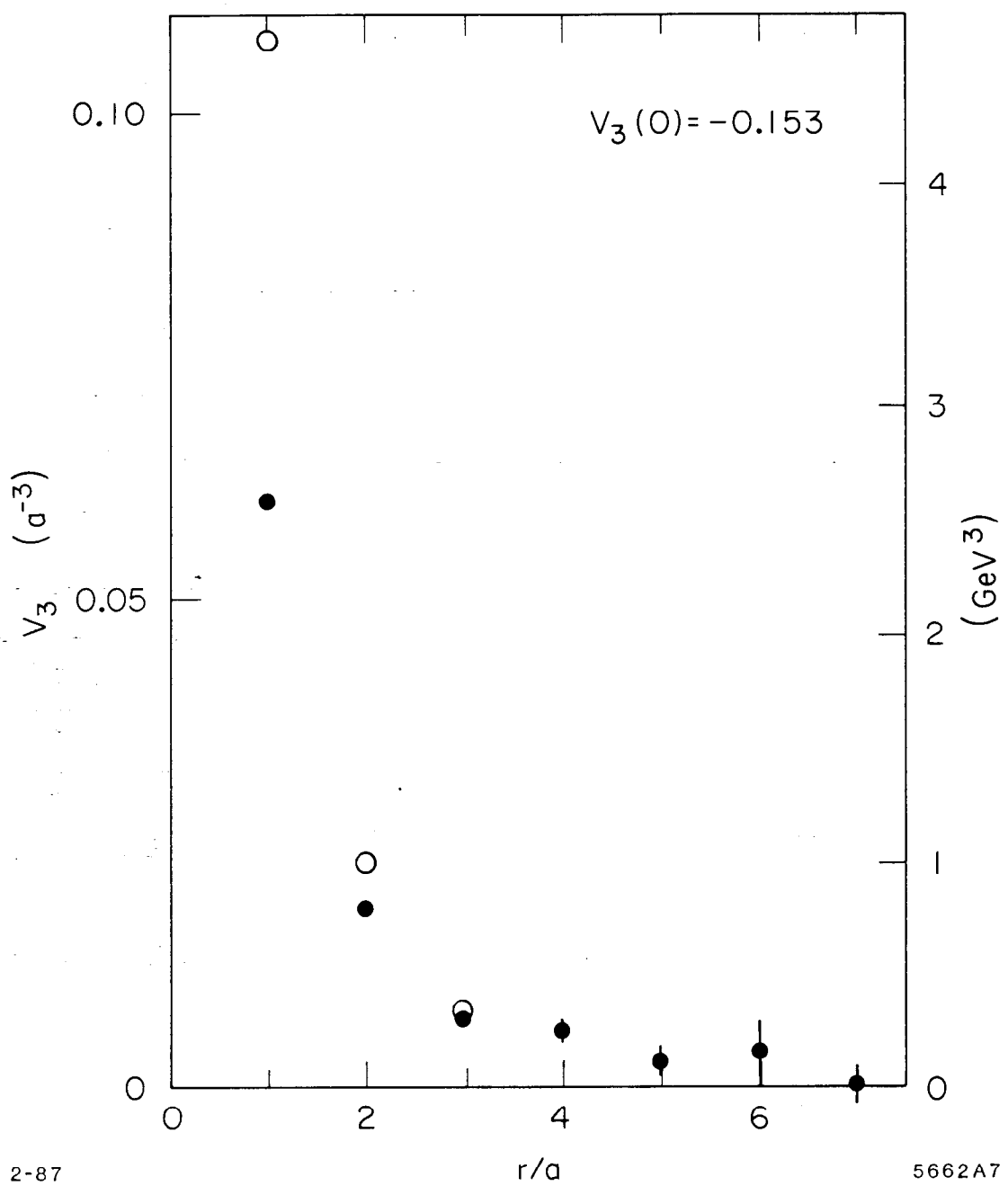

Fig. 10

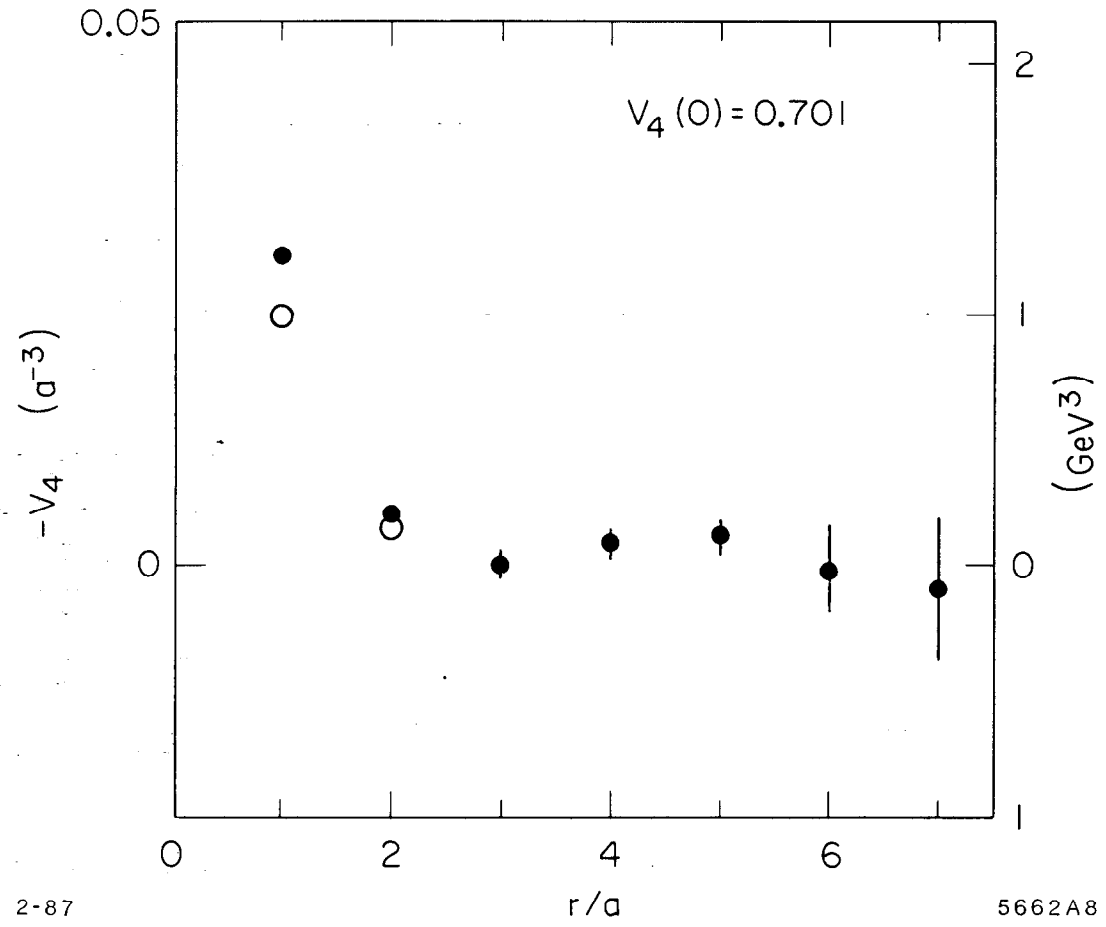

Fig. 11

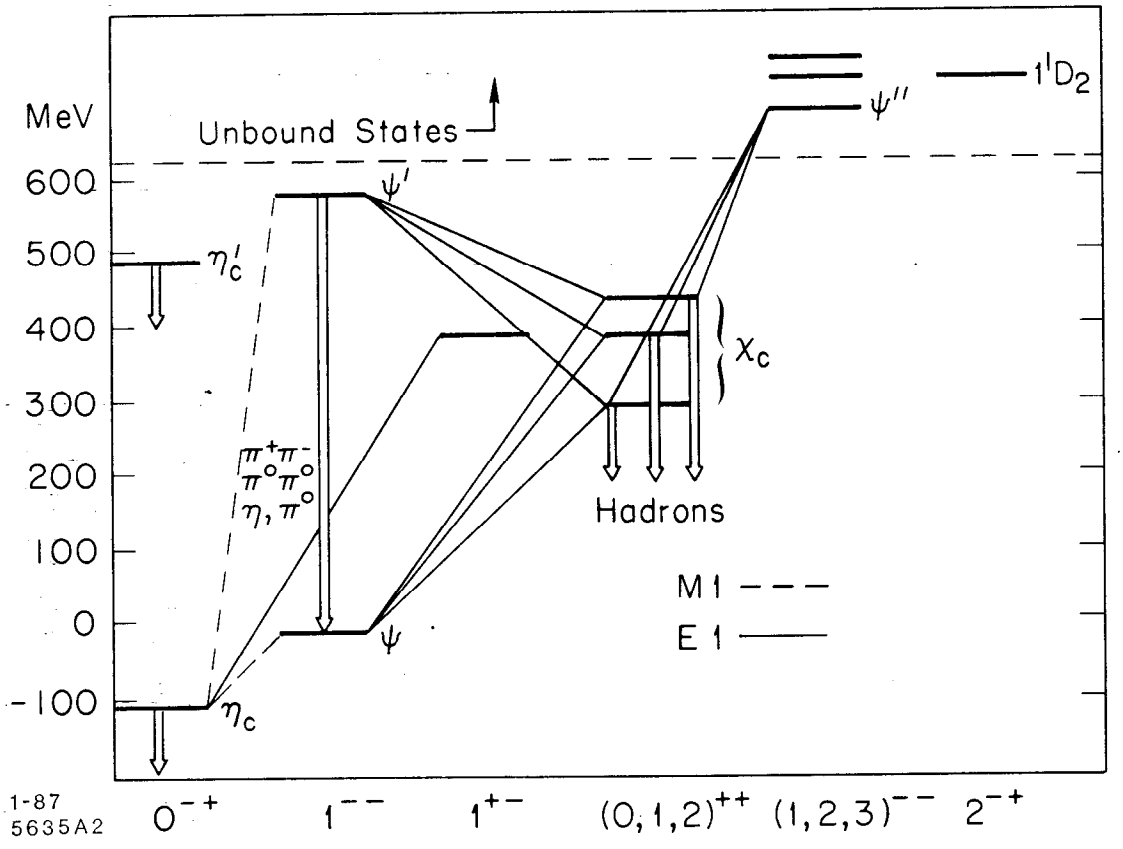
MeV
600
500
400
300
200
100
0
-100
Unbound States
ψ'
η_c'
$\pi^+\pi^-$
$\pi^0\pi^0$
η, π^0
η_c
ψ
ψ''
1^1D_2
χ_c
Hadrons
M1 - - -
E1 ——
1-87
5635A2
0^{-+}
1^{--}
1^{+-}
$(0,1,2)^{++}$
$(1,2,3)^{--}$
2^{-+}

Fig. 12

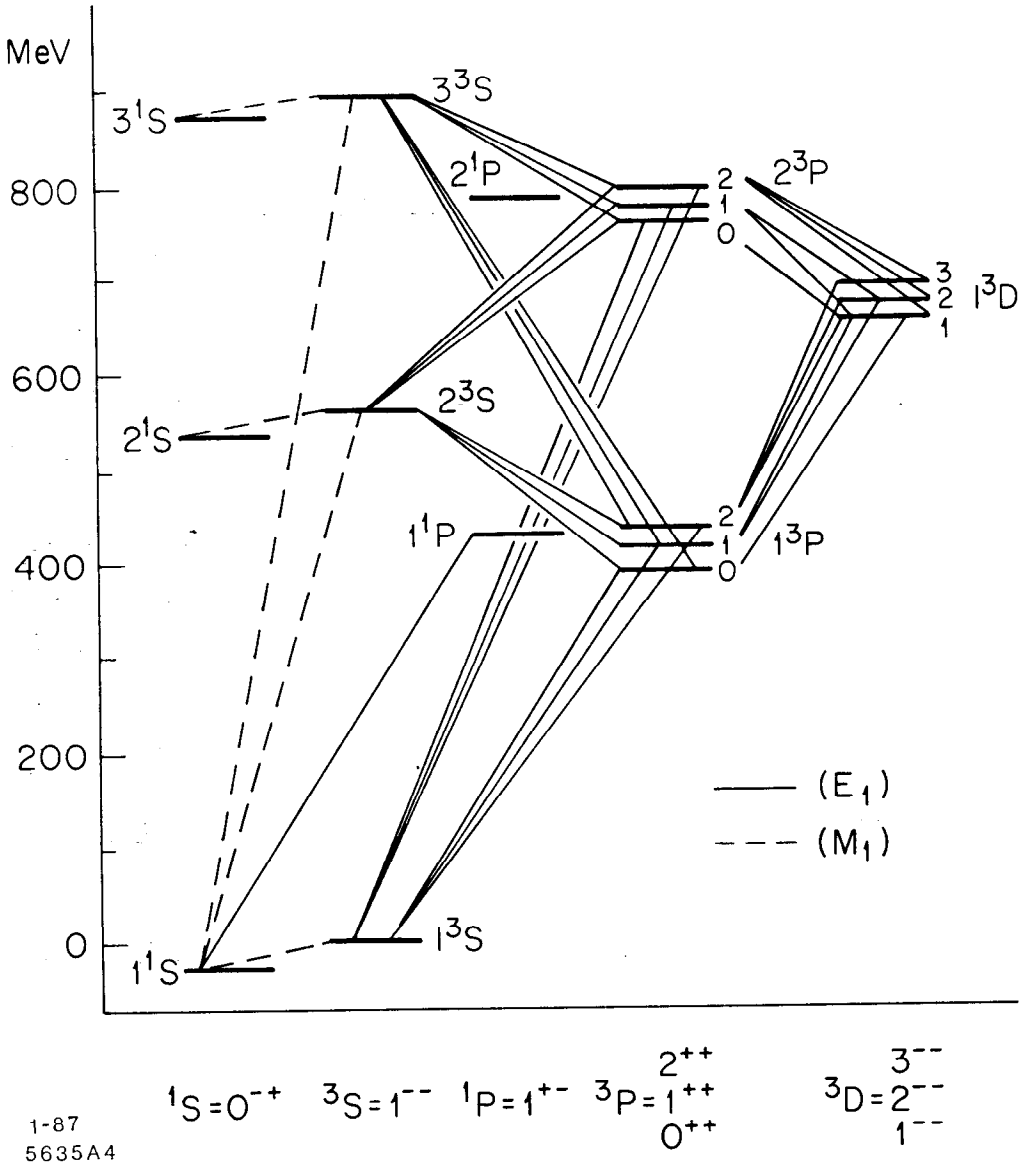
MeV
800
600
400
200
0
3^1S
2^1S
1^1S
3^3S
2^3S
1^3S
2^1P
1^1P
2^3P
1^3P
1^3D
2
1
0
3
2
1
(E_1)
(M_1)
$^1S = 0^{-+}$
$^3S = 1^{--}$
$^1P = 1^{+-}$
$^3P = 2^{++}\ 1^{++}\ 0^{++}$
$^3D = 3^{--}\ 2^{--}\ 1^{--}$
1-87
5635A4

Fig. 13

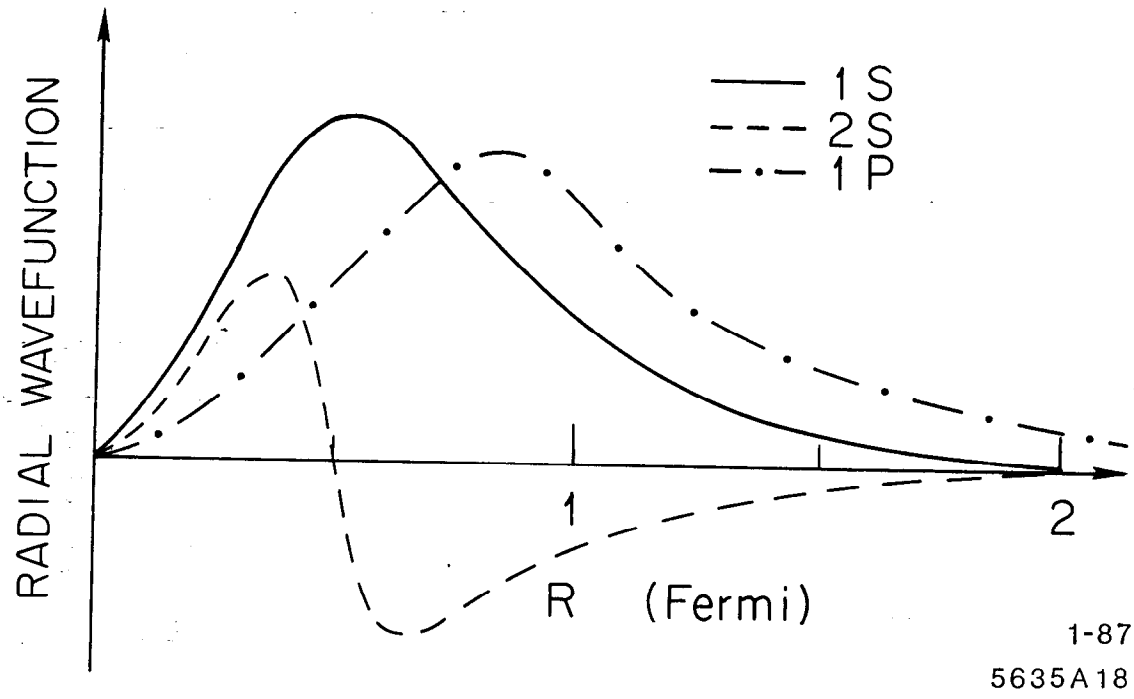

Fig. 14

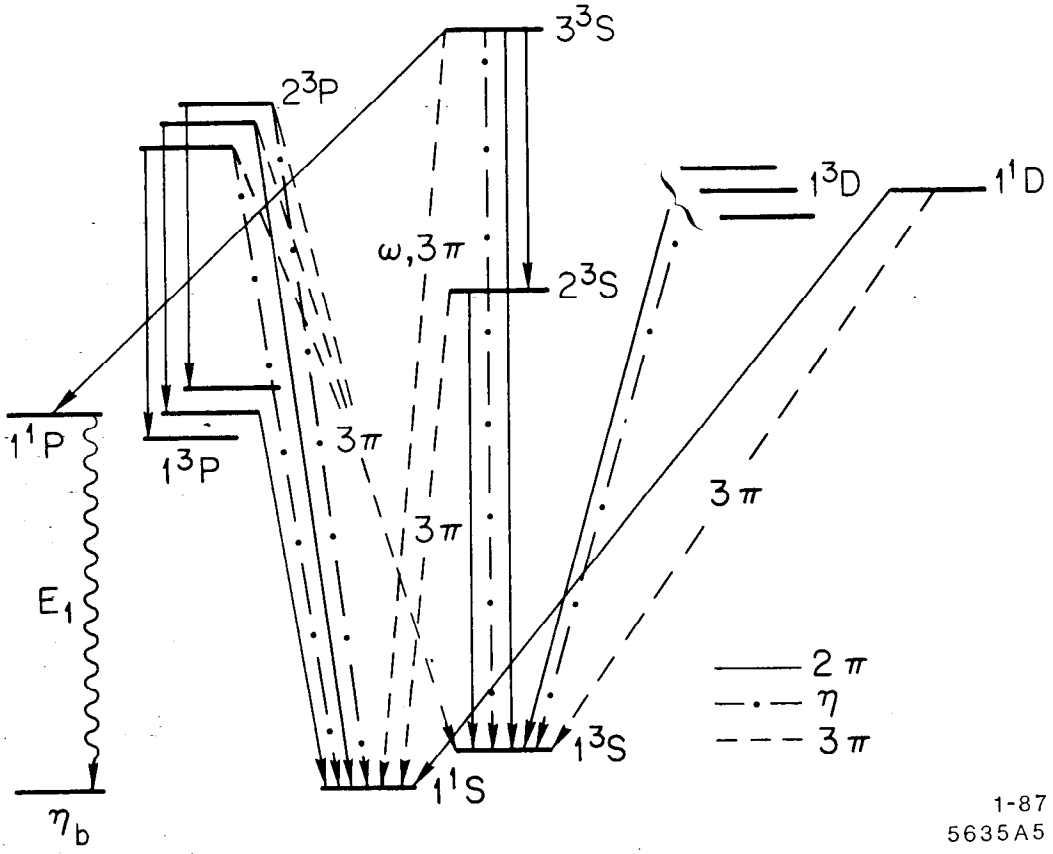
3^3S
2^3P
1^3D
1^1D
$\omega, 3\pi$
2^3S
1^1P
1^3P
3π
3π
3π
E_1
2π
η
3π
1^3S
1^1S
η_b
1-87
5635A5

Fig. 15

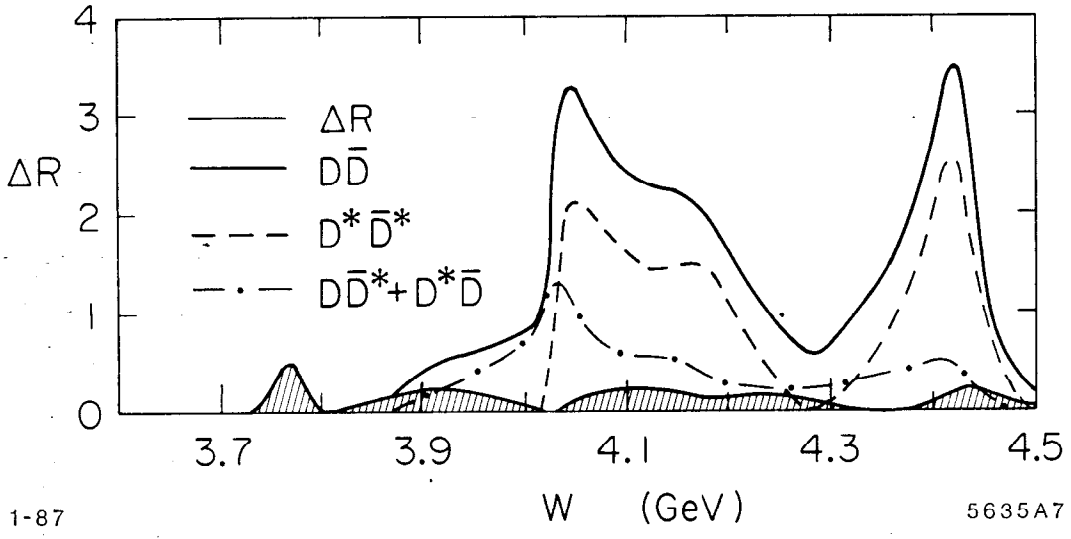

Fig. 16

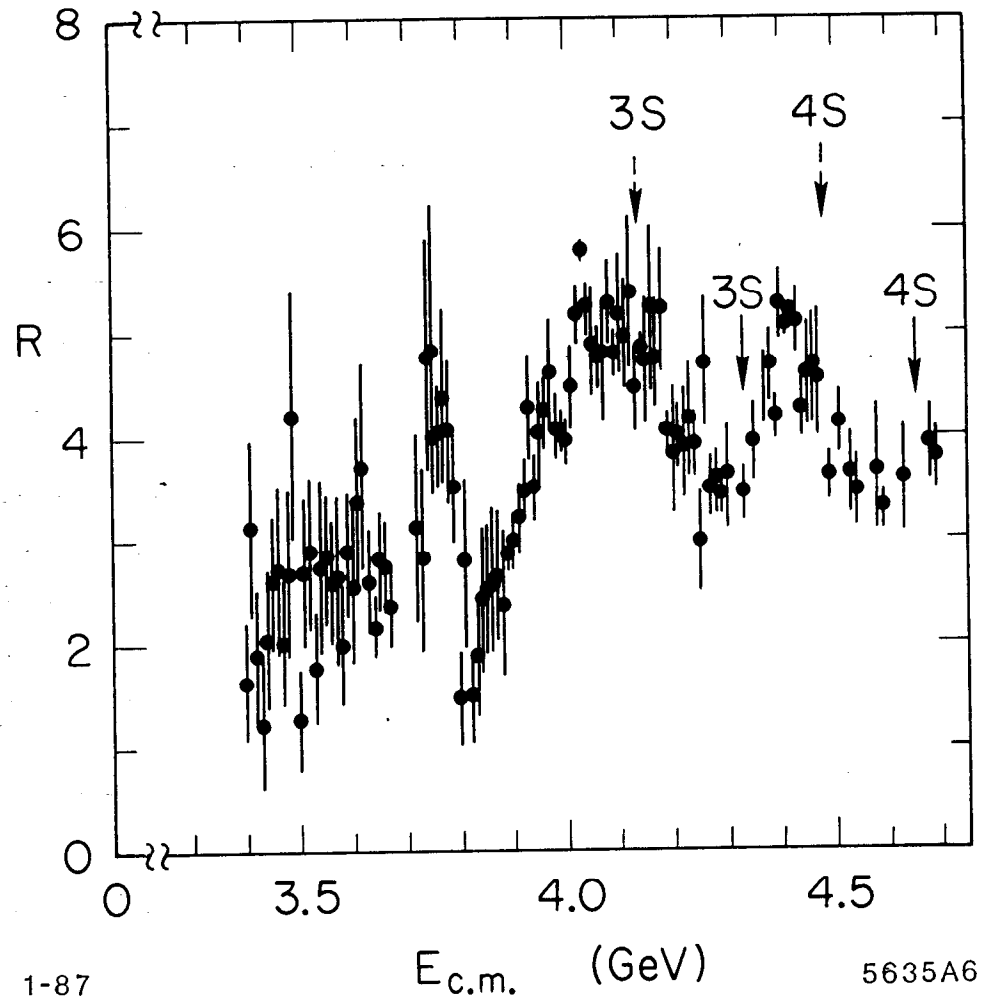

Fig. 17